A link between mitotic entry and membrane growth suggests a novel model for cell size control

Steph D. Anastasia, Duy Linh Nguyen, Vu Thai, Melissa Meloy, Tracy MacDonough, and Douglas R. Kellogg

Department of Molecular, Cell, and Developmental Biology, University of California, Santa Cruz, Santa Cruz, CA 95064

Addition of new membrane to the cell surface by membrane trafficking is necessary for cell growth. In this paper, we report that blocking membrane traffic causes a mitotic checkpoint arrest via Wee1-dependent inhibitory phosphorylation of Cdk1. Checkpoint signals are relayed by the Rho1 GTPase, protein kinase C (Pkc1), and a specific form of protein phosphatase 2A ($PP2A^{Cdc55}$). Signaling via this pathway is dependent on membrane traffic and appears to increase gradually during polar bud growth. We hypothesize that delivery of vesicles to the site of bud growth generates a signal that is proportional to the extent of polarized membrane growth and that the strength of the signal is read by downstream components to determine when sufficient growth has occurred for initiation of mitosis. Growth-dependent signaling could explain how membrane growth is integrated with cell cycle progression. It could also control both cell size and morphogenesis, thereby reconciling divergent models for mitotic checkpoint function.

Introduction

Eukaryotic cells show extraordinary diversity in size and shape, and they can maintain the same size even as their rate of growth changes. The mechanisms that underlie size control are largely unknown. It seems likely that these mechanisms are as ancient and conserved as the cell cycle because they would have been necessary for survival of the earliest eukaryotic cells. If so, there must be universal mechanisms for cell size control that are robust and adaptable so that they can function in cells of diverse shape and in cells that differ by many orders of magnitude in size. Although several proteins are known to be required for cell size control, it has not yet been possible to identify conserved core mechanisms that control cell size (Jorgensen and Tyers, 2004).

Cell size checkpoints play an important role in cell size control (Rupes, 2002; Kellogg, 2003; Jorgensen and Tyers, 2004). These checkpoints ensure that key cell cycle transitions are initiated only when sufficient growth has occurred. A cell size checkpoint that operates at entry into mitosis is thought to be mediated by the Wee1 kinase and the Cdc25 phosphatase (Nurse, 1975; Nurse et al., 1976). Wee1 delays mitosis by phosphorylating and inhibiting Cdk1 (Gould and Nurse, 1989). Cdc25 promotes entry into mitosis by removing the inhibitory phosphorylation (Russell and Nurse, 1986; Dunphy and Kumagai, 1991; Gautier et al., 1991; Kumagai and Dunphy, 1991). Early work in fission yeast discovered that Wee1 mutants enter mitosis before sufficient growth has occurred, leading to abnormally small cells (Nurse, 1975). Conversely, Cdc25 mutants delay entry into mitosis and become abnormally large (Nurse, 1975; Russell and Nurse, 1986). These observations led to the hypothesis that Wee1 delays mitosis until cells have reached a critical size.

The budding yeast homologues of Wee1 and Cdc25 are called Swe1 and Mih1. Loss of Swe1 causes premature mitosis and a reduced cell size (Lim et al., 1996; Jorgensen et al., 2002; Harvey and Kellogg, 2003; Harvey et al., 2005; Rahal and Amon, 2008). Loss of Mih1 causes delayed mitosis and an increased size (Russell et al., 1989; Jorgensen et al., 2002; Pal et al., 2008). Thus, the key functions of Wee1 and Cdc25 in fission yeast have been conserved in budding yeast, which suggests the existence of a conserved checkpoint. However, a role for Wee1 and Cdc25 family members in cell size control has been controversial because mutants may cause cell size defects indirectly by allowing more or less time for growth before entry into mitosis. Moreover, an alternative model has been proposed in which Wee1 and Cdc25 family members mediate a morphogenesis checkpoint that monitors the shape of the cell via the actin cytoskeleton (Lew and Reed, 1995a; Gachet et al., 2001; Lew, 2003; McNulty and Lew, 2005). The checkpoint functions of

Correspondence to Douglas R. Kellogg: dkellogg@ucsc.edu

The Rockefeller University Press $30.00
J. Cell Biol. Vol. 197 No. 1 89–104
www.jcb.org/cgi/doi/10.1083/jcb.201108108

Wee1 and Cdc25 are uncertain because we lack a clear understanding of the upstream signals that control their activity. Elucidation of these signals is thus an essential step toward understanding G2/M checkpoints and conserved mechanisms that control entry into mitosis.

Recent work has led to a new understanding of the function and regulation of Wee1 and Cdc25 family members. In both vertebrates and yeast, Wee1 and Cdc25 function in a systems-level mechanism that generates and maintains a low level of Cdk1 activity during early mitosis (Deibler and Kirschner, 2010; Harvey et al., 2011). The underlying mechanism is best understood in yeast. Swe1 is initially phosphorylated by Cdk1 associated with mitotic cyclins, which stimulates Swe1 to bind, phosphorylate, and inhibit Cdk1 (Harvey et al., 2005, 2011). The initial phosphorylation of Swe1 is opposed by protein phosphatase 2A associated with the Cdc55 regulatory subunit ($PP2A^{Cdc55}$; Harvey et al., 2011). The opposing activity of $PP2A^{Cdc55}$ sets a threshold that limits activation of Wee1 by Cdk1, thereby allowing a low level of Cdk1 activity to escape Wee1 inhibition in early mitosis. A key early mitotic event that is initiated via low level activation of Cdk1 is a positive feedback loop in which Cdk1 promotes transcription of the mitotic cyclin Clb2, which leads to a rapid rise in Clb2 levels (Amon et al., 1993; Harvey et al., 2011). A second key event is a switch in the pattern of bud growth. Growth of the bud initially occurs in a polar manner, but when the mitotic cyclins appear, they trigger a switch to isotropic growth, in which growth occurs over the entire surface of the bud (Lew and Reed, 1993). The mitotic cyclins induce this switch by repressing transcription of the G1 cyclins Cln1 and Cln2, which drive polar bud growth (Lew and Reed, 1993; Amon et al., 1994; McCusker et al., 2007).

After the initial phosphorylation of Swe1 in early mitosis, subsequent phosphorylation events lead to full hyperphosphorylation of Swe1, which inactivates Swe1 and is likely necessary for full entry into mitosis (Harvey et al., 2005). In vertebrates and yeast, mitotic Cdk1 is capable of full hyperphosphorylation and inactivation of Wee1 family members when it is present at sufficiently high levels (Tang et al., 1993; Mueller et al., 1995; Harvey et al., 2005). However, multiple kinases are required for full hyperphosphorylation of Wee1 family members in vivo, and their relative contributions are poorly understood (Coleman et al., 1993; Wu and Russell, 1993; Shulewitz et al., 1999; Sreenivasan and Kellogg, 1999; Sakchaisri et al., 2004; Asano et al., 2005).

Cdc25 family members are also regulated by phosphorylation. Phosphorylation of vertebrate Cdc25 by mitotic Cdk1 stimulates Cdc25 activity in a feedback loop that promotes entry into mitosis (Kumagai and Dunphy, 1992; Izumi and Maller, 1993). A similar feedback loop may also work on Mih1 in budding yeast (Pal et al., 2008). Mih1 is also controlled by casein kinase 1, which is encoded by a pair of redundant genes called *YCK1* and *YCK2* (Pal et al., 2008). Early in the cell cycle, Mih1 undergoes hyperphosphorylation that is dependent on Yck1/2. During entry into mitosis, Yck1/2-dependent phosphorylation of Mih1 is removed by $PP2A^{Cdc55}$. A pair of redundant regulatory proteins called Zds1 and Zds2 bind to $PP2A^{Cdc55}$ and target it to Mih1 but are not required for the activity of $PP2A^{Cdc55}$ against Swe1 (Wicky et al., 2011). A model that could explain these observations is that hyperphosphorylation of Mih1 early in the cell cycle reflects the action of a checkpoint that keeps Mih1 inactive before mitosis. In this model, dephosphorylation of Mih1 by $PP2A^{Cdc55}$ relieves inhibition of Mih1 to promote mitotic entry. Although it has not yet been possible to assay the activity of differently phosphorylated forms of Mih1, genetic data support the idea that hyperphosphorylation of Mih1 is inhibitory (Pal et al., 2008; Wicky et al., 2011).

The dramatic cell cycle–dependent changes in phosphorylation of Mih1 and Swe1 likely reflect the action of upstream checkpoint signals that control their activity, yet the cellular events that send checkpoint signals to Mih1 and Swe1 are poorly understood. Here, we have explored the cellular events that send checkpoint signals to Mih1 and Swe1. A starting point for these analyses was the connection between Yck1/2 and Mih1. We found this connection to be intriguing because Yck1/2 are transported to the site of bud growth on secretory vesicles (Babu et al., 2002). Moreover, inactivation of Yck1/2 causes defects in bud growth and Cdk1 inhibitory phosphorylation (Robinson et al., 1993; Pal et al., 2008). These observations suggested that control of Cdk1 inhibitory phosphorylation could be linked to membrane traffic. In principle, mechanisms that link cell cycle progression to membrane traffic must exist to ensure that growth is coordinated with the cell cycle. We therefore set out to test for a connection between membrane traffic and control of Mih1 and Swe1.

Results

Blocking membrane traffic triggers a rapid Swe1-dependent checkpoint arrest

We analyzed the effects of disrupting membrane traffic on progression through mitosis in synchronized rapidly dividing cells. To disrupt membrane traffic, we used a temperature-sensitive mutant of *SEC6* (*sec6-4*) because previous work found that it causes a rapid arrest of membrane traffic. Sec6 is a component of the exocyst complex, which is required for docking and fusion of secretory vesicles at the site of membrane growth in the bud (TerBush et al., 1996). To assess mitotic progression, we assayed cleavage of the cohesin Mcd1, which normally occurs at the metaphase to anaphase transition, as well as levels of the mitotic cyclin Clb2.

Wild-type and *sec6-4* cells were released from a G1 arrest and shifted to the restrictive temperature at 30 min after release, which was before bud growth had been initiated. Growth of a new bud was blocked in *sec6-4* cells because membrane traffic is required for bud growth. Mcd1 cleavage failed to occur in *sec6-4* cells, which indicated that they arrested before anaphase (Fig. 1 A). To determine whether the arrest was caused by Swe1-dependent inhibitory phosphorylation of Cdk1, we also assayed Mcd1 cleavage in *sec6-4 swe1Δ* cells (Fig. 1 A). The extent and timing of Mcd1 cleavage were similar in wild-type and *sec6-4 swe1Δ* cells, which revealed that *swe1Δ* caused complete checkpoint failure. As expected, the *sec6-4* cells

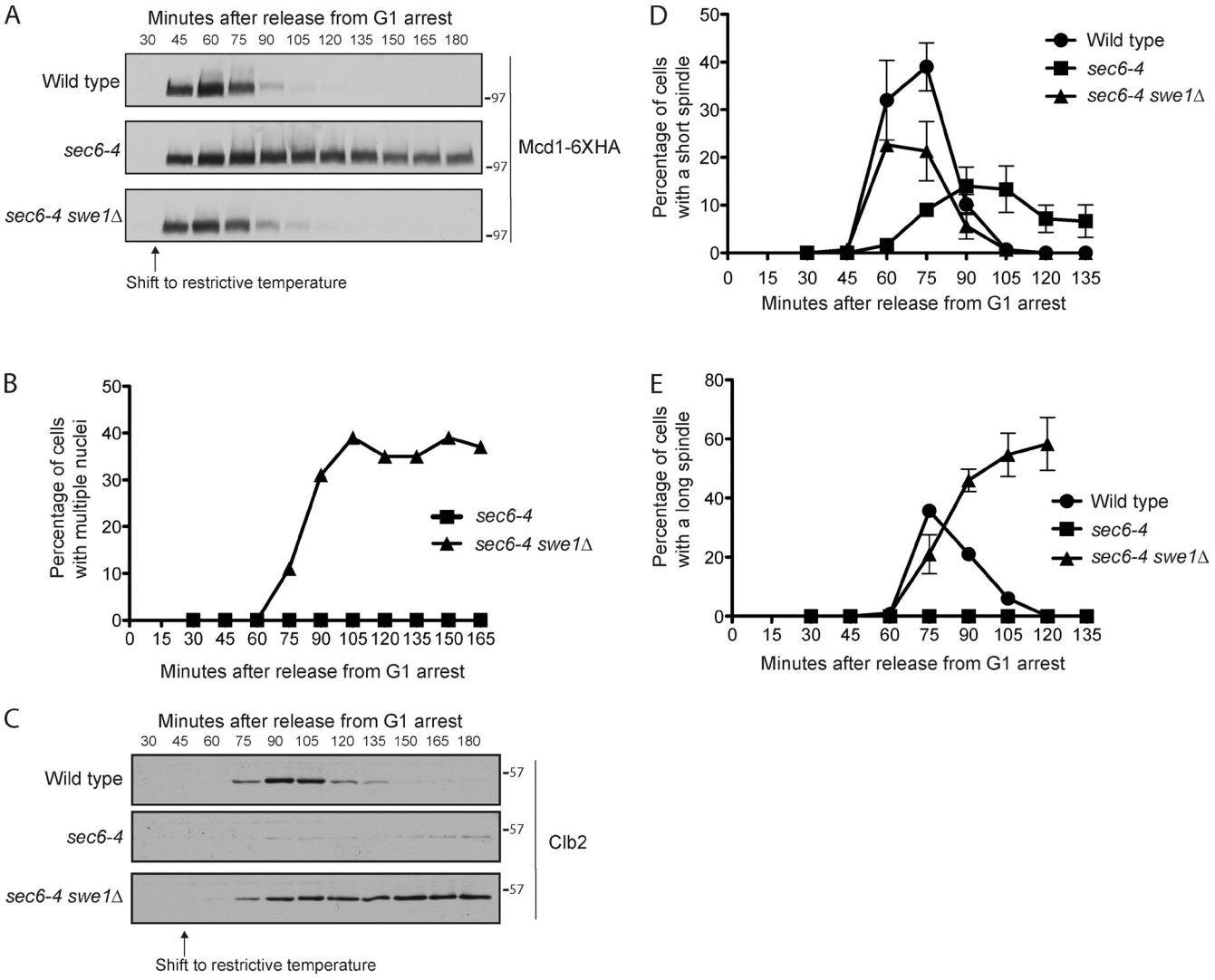

Figure 1. **Blocking membrane traffic triggers a checkpoint arrest.** (A) Cells were released from a G1 arrest and shifted to the restrictive temperature (34°C) at 30 min after release. Cleavage of Mcd1-6×HA was assayed by Western blotting. (B) Cells were released from a G1 arrest and shifted to the restrictive temperature (34°C) at 30 min after release. DNA staining was used to determine the percentage of cells with multiple nuclei. (C) Cells were released from a G1 arrest and shifted to the restrictive temperature (34°C) at 45 min after release. Levels of Clb2 were assayed by Western blotting. (D and E) Cells were released from a G1 arrest and shifted to the restrictive temperature (34°C) at 30 min after release. The percentage of cells with short or long spindles was determined. Error bars represent SEMs for three biological replicates. Numbers shown next to the Western blots indicate molecular mass in kilodaltons.

arrested with a single nucleus, whereas the *sec6-4 swe1Δ* cells underwent nuclear division within the unbudded mother cell to form binucleate cells (Fig. 1 B).

To further characterize the arrest, we analyzed accumulation of the mitotic cyclin Clb2. The *sec6-4* mutant caused a severe delay in Clb2 accumulation that was rescued by *swe1Δ* (Fig. 1 C). We also analyzed mitotic spindles. In budding yeast, assembly of a short mitotic spindle is initiated in early mitosis by a low level of mitotic Cdk1 activity (Rahal and Amon, 2008). During anaphase, the spindle elongates to segregate the chromosomes. The *sec6-4* mutant caused delayed and reduced assembly of short spindles as well as a complete block to spindle elongation (Fig. 1, D and E). Clb2 levels remained elevated, and long spindles did not disassemble normally in *sec6-4 swe1Δ* cells, which may be caused by a checkpoint that prevents exit from mitosis when cytokinesis is blocked by a checkpoint that monitors spindle orientation in the daughter bud (Balasubramanian et al., 2000; Pereira et al., 2000). Membrane traffic is required for cytokinesis (Xu et al., 2002).

Together, these observations demonstrate that blocking membrane traffic triggers a Swe1-dependent checkpoint arrest. They also suggest that the checkpoint blocks low level activation of Cdk1 in early mitosis, which leads to a failure in short spindle assembly and a failure to activate the positive feedback loop that promotes Clb2 transcription (Amon et al., 1993).

Normal signaling to Mih1 and Swe1 fails to occur when membrane traffic is blocked

A cell cycle arrest could be induced by preventing activation of Mih1, inactivation of Swe1, or both. We therefore tested whether blocking membrane traffic sends signals to Mih1 or Swe1. Mih1 and Swe1 undergo dramatic changes in phosphorylation

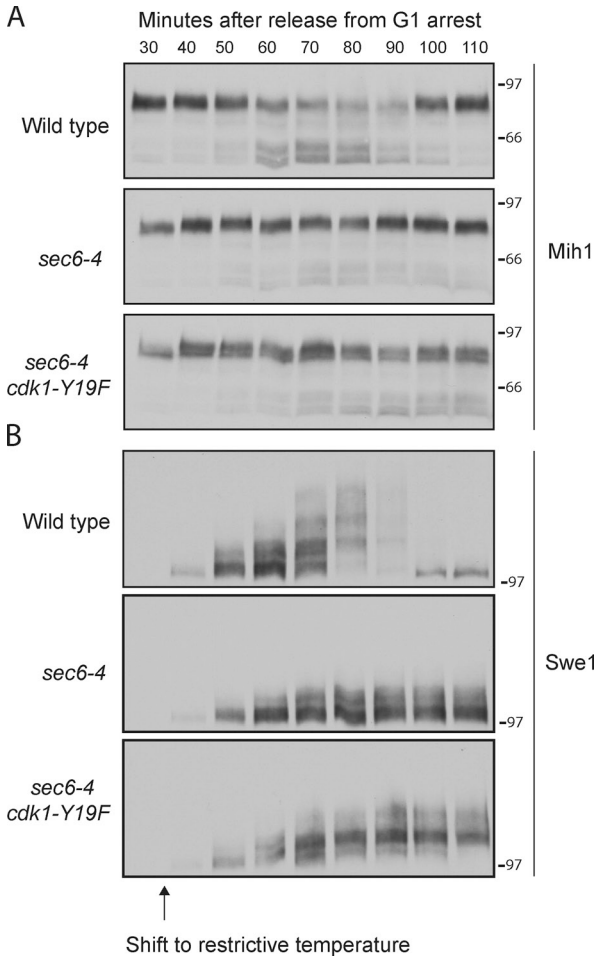

Figure 2. **Normal signaling to Mih1 and Swe1 fails to occur when membrane traffic is blocked.** (A and B) Cells were released from a G1 arrest and shifted to the restrictive temperature (34°C) at 30 min after release. The behavior of Mih1 and Swe1 were assayed by Western blotting. Numbers shown next to the Western blots indicate molecular mass in kilodaltons.

during entry into mitosis that provide a readout for signals that control their activity or localization (Sreenivasan and Kellogg, 1999; Harvey et al., 2005; Pal et al., 2008). Phosphorylation of Swe1 and Mih1 can be assayed by Western blotting, which detects shifts in their electrophoretic mobility. In principle, changes in phosphorylation of Mih1 or Swe1 during a checkpoint arrest could be a cause of the arrest, or they could be an indirect consequence of the arrest. To test for the latter possibility, we included a control in which phosphorylation of Swe1 and Mih1 was assayed in *sec6-4 cdk1-Y19F* cells. The *cdk1-Y19F* allele lacks the conserved tyrosine that is targeted by Swe1, so cells carrying this allele fail to undergo checkpoint arrest.

Wild-type, *sec6-4*, and *sec6-4 cdk1-Y19F* cells were released from a G1 arrest and shifted to the restrictive temperature at 30 min after release. The dephosphorylation of Mih1 that normally occurs during entry into mitosis failed to occur normally in *sec6-4* cells (Fig. 2 A). Limited dephosphorylation of Mih1 occurred in *sec6-4 cdk1-Y19F* cells, but it was delayed and diminished. Swe1 underwent partial hyperphosphorylation in *sec6-4* and *sec6-4 cdk1-Y19F* cells but failed to undergo the normal full hyperphosphorylation that is associated with inactivation of Swe1 (Fig. 2 B). It also failed to undergo destruction. The partial phosphorylation of Swe1 observed in *sec6-4* and *sec6-4 cdk1-Y19F* cells likely corresponds to the initial activation of Swe1 by Cdk1 that occurs during entry into mitosis (Harvey et al., 2005, 2011).

Wee1 family members are inactivated when they are fully hyperphosphorylated, and it is thought that dephosphorylation of Mih1 plays a role in its activation (Mueller et al., 1995; Harvey et al., 2005; Pal et al., 2008; Wicky et al., 2011). Thus, these observations suggest that the checkpoint blocks entry into mitosis by coordinately preventing inactivation of Swe1 and activation of Mih1.

Blocking membrane traffic during early mitosis triggers rapid signaling to Mih1

We next examined the effects of inactivating membrane traffic during early mitosis. Wild-type and *sec6-4* cells were released from a G1 arrest and shifted to the restrictive temperature at 70 min after release. At this time, bud emergence was complete, and Mih1 dephosphorylation was just beginning. Because Mih1 dephosphorylation is initiated when the mitotic cyclin Clb2 first appears, the presence of dephosphorylated forms of Mih1 indicated that cells were initiating the G2 to M transition (Pal et al., 2008). Blocking membrane traffic at this point caused rapid reversal of Mih1 dephosphorylation (Fig. 3 A). The response was remarkably rapid: Mih1 hyperphosphorylation was complete within 5 min. The response time includes the time required for the cultures to reach the restrictive temperature and for protein inactivation to occur, so it is likely that the actual response time is even more rapid. Inactivation of *sec6-4* at this time did not cause a rapid change in Swe1 phosphorylation, although at the time of the temperature shift, Swe1 was in the partially phosphorylated active form and had not yet undergone full hyperphosphorylation that is associated with Swe1 inactivation.

The rapid hyperphosphorylation of Mih1 was not affected by the *cdk1-Y19F* allele, which indicated that it was caused by signals upstream of Mih1 (Fig. 3 A). Dephosphorylated forms of Mih1 reappeared in *sec6-4 cdk1-Y19F* cells at longer times after the shift to the restrictive temperature. This is consistent with the experiment in Fig. 2 A, which showed that dephosphorylated forms of Mih1 appear in later time points in *sec6-4 cdk1-Y19F* cells shifted to the restrictive temperature in G1. One explanation for these observations is that mitotic Cdk1 activity may trigger a positive feedback loop that contributes to Mih1 dephosphorylation, but only when it reaches high levels.

To test whether rapid hyperphosphorylation of Mih1 is a general response to an arrest of secretion, we tested a mutant that affects intra-Golgi transport (*sec7-4*). The *sec7-4* mutant caused hyperphosphorylation of Mih1 as rapidly as the *sec6-4* mutant (Fig. 3 B). We also tested mutants that affect endocytosis, including a conditional allele of *END3* (*end3-1*) and deletions of *SYP1* and *EDE1*. None of the mutants caused hyperphosphorylation of Mih1.

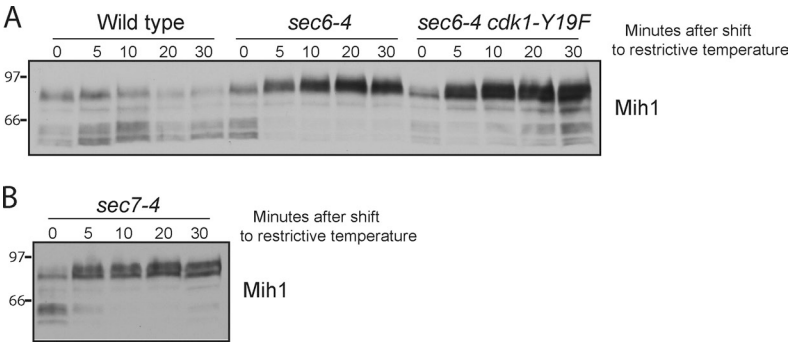

Figure 3. **Blocking membrane traffic triggers rapid signaling to Mih1.** (A and B) Cells were released from a G1 arrest and were shifted to the restrictive temperature (34°C) at 70 min after release, when Mih1 dephosphorylation was being initiated. Mih1 phosphorylation was assayed by Western blotting. Numbers shown next to the Western blots indicate molecular mass in kilodaltons.

The effects of blocking membrane traffic do not appear to be caused by indirect effects on actin

Previous work reached the conclusion that Swe1 mediates a checkpoint that monitors bud morphogenesis. This was based on the observation that depolymerization of actin causes a Swe1-dependent checkpoint arrest (Lew and Reed, 1995a; Lew, 2003; Keaton and Lew, 2006). Because actin is required for bud morphogenesis, it was proposed that the checkpoint monitors bud morphogenesis. However, actin is required for delivery of vesicles to the growing bud, and depolymerization of actin therefore causes rapid cessation of growth (Mulholland et al., 1997; Karpova et al., 2000). Thus, depolymerization of actin could activate a checkpoint arrest indirectly by blocking membrane traffic. Conversely, blocking membrane traffic causes defects in actin organization, which suggests that blocking membrane traffic could cause a checkpoint arrest indirectly by causing defects in actin organization (Finger and Novick, 1997; Pruyne et al., 2004).

To learn more about the relative effects of depolymerizing actin versus blocking membrane traffic, we tested whether actin depolymerization caused rapid hyperphosphorylation of Mih1. Wild-type cells were released from a G1 arrest, and latrunculin A was added at 70 min after release to depolymerize actin. The effects on Mih1 phosphorylation were indistinguishable from the effects caused by blocking membrane traffic (Fig. 4 A).

We next tested whether blocking membrane traffic caused rapid defects in the organization of actin. Wild-type and *sec6-4* cells were shifted to the restrictive temperature, and phalloidin staining was used to monitor actin organization. There were no detectable effects on the organization of actin cables or patches after 5 min, when effects on Mih1 phosphorylation were maximal (Figs. 3 and 4 B).

Together, these observations suggest that the checkpoint arrest caused by actin depolymerization may be a consequence of a block to membrane traffic. However, we cannot rule out the possibility that *sec6-4* causes rapid defects in actin organization that cannot be detected by fluorescence microscopy.

Overexpression of Zds1 drives cells through the checkpoint arrest caused by blocking membrane traffic

We next searched for the signals that control Swe1 and Mih1 in response to arrest of membrane traffic. $PP2A^{Cdc55}$ was a good candidate because it controls both Swe1 and Mih1 (Lin and Arndt, 1995; Minshull et al., 1996; Yang et al., 2000; Pal et al., 2008; Yasutis et al., 2010; Harvey et al., 2011; Wicky et al., 2011). $PP2A^{Cdc55}$ is regulated by a pair of redundant proteins called Zds1 and Zds2 that associate with $PP2A^{Cdc55}$ and target it to Mih1 (Queralt and Uhlmann, 2008; Yasutis et al., 2010; Wicky et al., 2011). It appears that Zds1/2 can play both activating and inhibitory roles in regulation of $PP2A^{Cdc55}$ (Pal et al., 2008; Queralt and Uhlmann, 2008). There are also hints that Zds1/2 inhibit the activity of $PP2A^{Cdc55}$ against Swe1 (Wicky et al., 2011).

Previous work found that overexpression of Zds2 can override the checkpoint arrest caused by depolymerization of actin (Yasutis et al., 2010). The ability of Zds2 to override the checkpoint was dependent on Cdc55, which indicated that it works through $PP2A^{Cdc55}$ (Yasutis et al., 2010). We found that overexpression of Zds1 drove cells through the checkpoint arrest caused by blocking membrane traffic, as revealed by cleavage of Mcd1 (Fig. 5 A). Moreover, overexpression of

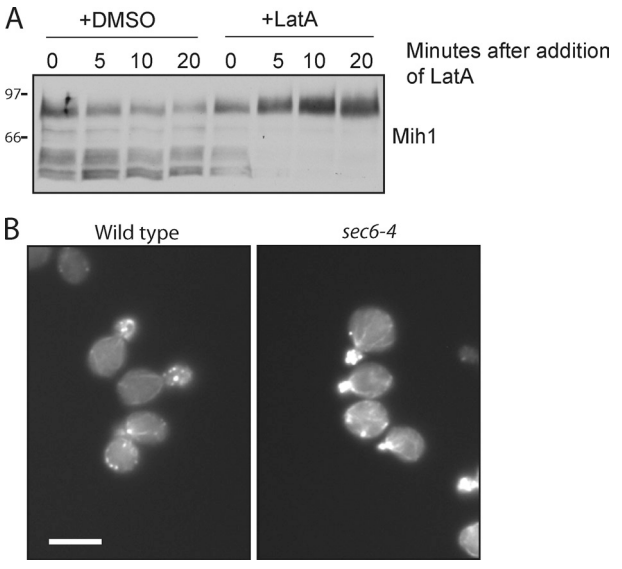

Figure 4. **The response to arrest of membrane traffic is not a consequence of indirect effects on actin.** (A) Wild-type cells were released from a G1 arrest at room temperature. A sample was taken at 70 min after release (t = 0), and the cells were divided into two aliquots. Latrunculin A (LatA) was added to one aliquot, and solvent (DMSO) was added to the other as a control. Mih1 phosphorylation was assayed by Western blotting. (B) Cells were grown to log phase in YPD media and then shifted to the restrictive temperature (34°C) for 5 min. Cells were then fixed and stained with FITC-phalloidin. Bar, 5 µm. Numbers shown next to the Western blot indicate molecular mass in kilodaltons.

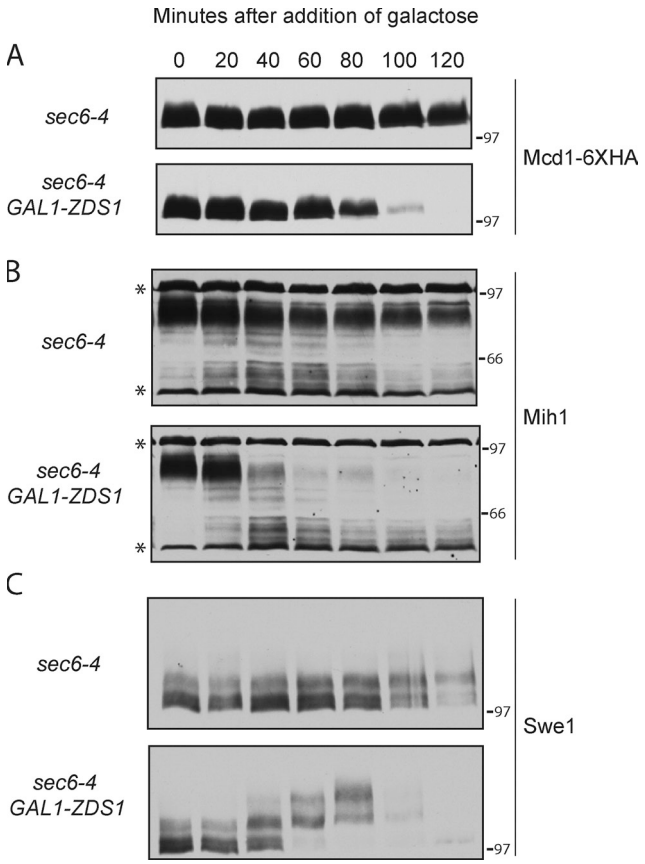

Figure 5. **Overexpression of Zds1 drives cells through the checkpoint arrest.** (A–C) Cells were grown in YEP with 2% raffinose and arrested in G1 with α-factor at 25°C. Cells were released from the arrest into YEP with 2% raffinose at 25°C. When 10% of cells had undergone bud emergence, they were shifted to the restrictive temperature (34°C) to induce the checkpoint arrest. After 30 min, galactose was added to induce expression of *ZDS1*. Cleavage of Mcd1-3×HA and phosphorylation of Mih1 and Swe1 were assayed by Western blotting. The asterisks denote background bands that appear with some batches of purified anti-Mih1 antibody. Numbers shown next to the Western blots indicate molecular mass in kilodaltons.

Zds1 in checkpoint-arrested cells caused dephosphorylation of Mih1 and hyperphosphorylation of Swe1 (Fig. 5, B and C). These observations suggest that $PP2A^{Cdc55}$ coordinately regulates Swe1 and Mih1 and that Zds1/2 are key regulators of the checkpoint functions of $PP2A^{Cdc55}$. An attractive model is that Zds1/2 coordinately regulate Swe1 and Mih1 by shifting the activity of $PP2A^{Cdc55}$ away from Swe1 to Mih1. This could initiate full hyperphosphorylation and inactivation of Swe1 as well as dephosphorylation of Mih1, which is likely necessary for Mih1 activation.

Pkc1 controls entry into mitosis

To better understand how arrest of membrane traffic triggers a checkpoint arrest, we searched for proteins that regulate $PP2A^{Cdc55}$-Zds1/2. Pkc1, the budding yeast member of the atypical PKC family, was a good candidate because it associates with Zds2 in a two-hybrid assay (Uetz et al., 2000; Drees et al., 2001; Yasutis et al., 2010). Moreover, Pkc1 functions in a signaling pathway that blocks ribosome biogenesis when membrane traffic is blocked, which demonstrates that it mediates a response to arrest of membrane traffic (Li et al., 2000; Nanduri and Tartakoff, 2001). Finally, the closest homologue of Pkc1 in vertebrates is PRK2 (PKC-related kinase 2). Depletion of PRK2 by RNAi causes a G2/M block, most likely due to a failure to properly regulate Cdc25 (Roelants et al., 2004; Schmidt et al., 2007). Pkc1 is localized to the site of membrane growth and is therefore well positioned to relay signals regarding the status of growth (Andrews and Stark, 2000).

We first used coimmunoprecipitation to confirm the reported two-hybrid interaction between Zds2 and Pkc1. Pkc1 could be coprecipitated with $PP2A^{Cdc55\text{-}3\times HA}$ in wild-type cells but not in *zds1Δ zds2Δ* cells, consistent with an interaction between Pkc1 and Zds1/2 (Fig. 6 A). Pkc1 was hyperphosphorylated in extracts made from *zds1Δ zds2Δ* cells, which suggests that $PP2A^{Cdc55}$ may oppose phosphorylation of Pkc1 (Fig. 6 A).

We next analyzed the effects of inactivating Pkc1. The commonly used temperature-sensitive allele of *PKC1* (*pkc1-1*) has a restrictive temperature of 37°C, which causes transient heat shock effects in wild-type cells that affect phosphorylation of Mih1 and Swe1. We therefore isolated a collection of 40 new *pkc1* temperature-sensitive alleles to find alleles that cause rapid inactivation of Pkc1 at 34°C, which does not cause heat shock effects. We also hoped to identify mutants that preferentially affect different functions of Pkc1, which could provide new information on Pkc1 function.

We first screened the collection of alleles for mutants that affect mitosis. We reasoned that if Pkc1 relays signals that inactivate Swe1 or activate Mih1, loss of Pkc1 could cause cells to become elongated because mitotic Cdk1 suppresses polar bud growth (Booher et al., 1993; Lew and Reed, 1995b; Ma et al., 1996). Five *pkc1* mutants caused a significant fraction of cells to become elongated when grown at semirestrictive temperatures. In each case, the elongated cell phenotype was eliminated by *swe1Δ*, which indicated that it was caused by a failure to control Cdk1 inhibitory phosphorylation. The strongest phenotype was observed in *pkc1-14* cells grown at a semirestrictive temperature of 30°C. The elongated phenotype became severe when cells were grown to high density, which suggests that *pkc1-14* compromises functions of Pkc1 that are important when growth is slowed by nutrient limitation (Fig. 6 B). *pkc1-14* was recessive to wild-type *PKC1*.

We next assayed Mih1 dephosphorylation in *pkc1-14* cells. Cells were released from a G1 arrest and shifted to the restrictive temperature at 75 min after release, when bud emergence was complete and cells were entering mitosis. Mih1 dephosphorylation failed to occur as Clb2 levels increased, consistent with a role for Pkc1 in controlling Mih1 phosphorylation (Fig. 6 C). In both wild-type and *pkc1-14* cells, Swe1 remained in the partially phosphorylated form. We were not able to analyze a more complete cell cycle in *pkc1* mutants because they caused cell lysis after longer times at the restrictive temperature, as reported previously for other *pkc1* alleles (Levin and Bartlett-Heubusch, 1992).

Pkc1 controls Mih1 phosphorylation via $PP2A^{Cdc55}$-Zds1

We next analyzed the effects of a *PKC1* gain-of-function allele. A constitutively active form of Pkc1 (referred to as Pkc1*) can be created by mutating an autoinhibitory phosphorylation site

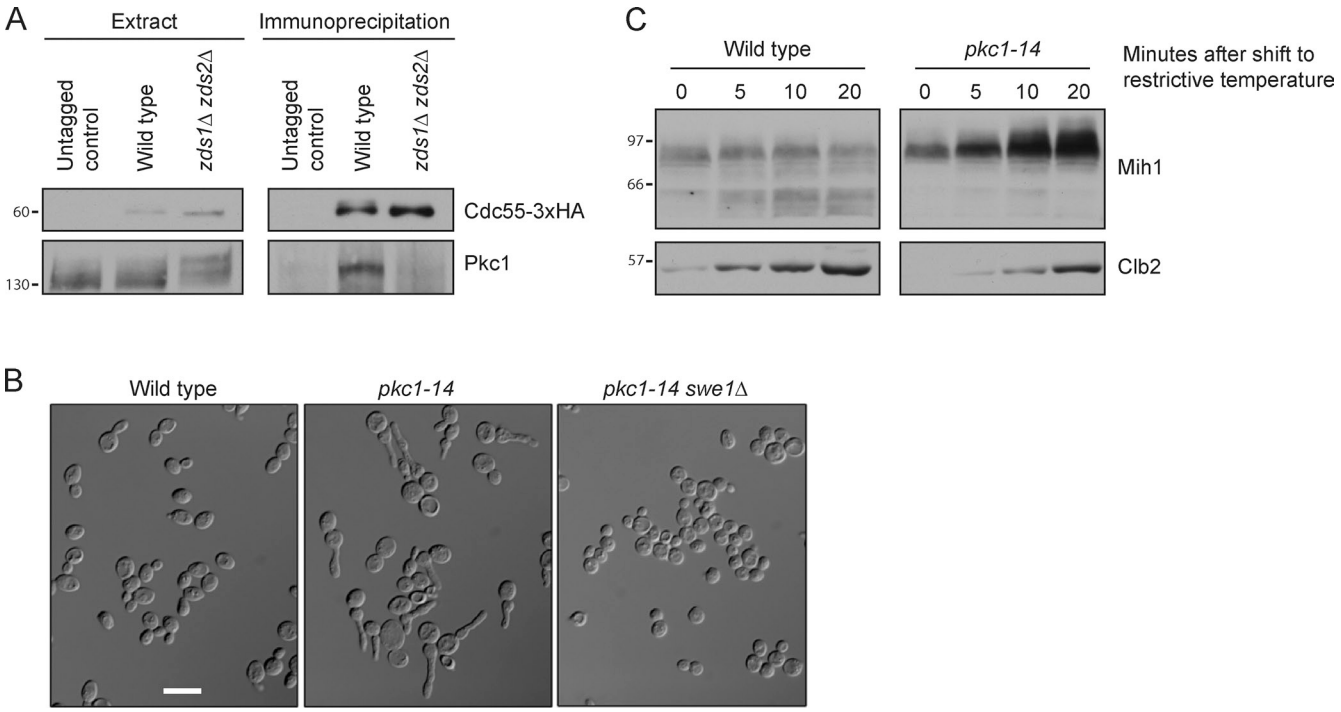

Figure 6. **Pkc1 associates with PP2A^{Cdc55} and is required for Mih1 dephosphorylation.** (A) Anti-HA antibodies were used to immunoprecipitate PP2A$^{Cdc55\text{-}3xHA}$ from wild-type, *zds1Δ zds2Δ*, and untagged control cells. Coprecipitation of Pkc1 was assayed by Western blotting with anti-Pkc1 antibodies. Crude extract samples were electrophoresed longer than the immunoprecipitated samples to resolve phosphorylation forms. (B) Cells were inoculated into YPD media at low density and grown at 30°C until they reached an OD of ∼1.7. Bar, 10 µm. (C) Cells were released from a G1 arrest and shifted to the restrictive temperature (34°C) at 75 min after release. Mih1 phosphorylation and Clb2 levels were assayed by Western blotting. Numbers shown next to the Western blots indicate molecular mass in kilodaltons.

(Watanabe et al., 1994). Expression of Pkc1* from the *GAL1* promoter caused rapid dephosphorylation of Mih1 (Fig. 7 A). Pkc1* did not cause dephosphorylation of Mih1 in cells carrying a temperature-sensitive allele of *CDC55* (*cdc55-4*), which demonstrated that it acts via PP2A^{Cdc55} (Fig. 7 B). Pkc1* was able to drive dephosphorylation of Mih1 in checkpoint-arrested cells (Fig. 7 C).

In previous work, we found that a fraction of Zds1 undergoes dephosphorylation during entry into mitosis (Wicky et al., 2011). Because Pkc1 associates with Zds1/2, we tested whether Pkc1* caused effects on Zds1 phosphorylation. We found that Pkc1* caused rapid dephosphorylation of Zds1 (Fig. 7 D). Together, the effects of loss-of-function and gain-of-function mutants demonstrate that Pkc1 relays signals via PP2A^{Cdc55}-Zds1/2 that control Mih1 phosphorylation and entry into mitosis.

Rho1 signals to Mih1 via Pkc1

An important upstream regulator of Pkc1 is the Rho1 GTPase; the active GTP-bound form of Rho1 directly binds and activates Pkc1 (Kamada et al., 1996). A previous study identified temperature-sensitive alleles of *RHO1* that appear to be defective in activation of Pkc1 (Saka et al., 2001). We assayed Mih1 phosphorylation in one of these alleles (*rho1-2*) and found that dephosphorylation of Mih1 failed to occur when cells were grown at a semirestrictive temperature (Fig. 8 A). A hyperphosphorylated form of Mih1 appeared in the *rho1-2* cells that was not detected in control cells, which is consistent with a role for Rho1 in activation of PP2A^{Cdc55} (Fig. 8 A, arrowhead). Full hyperphosphorylation of Swe1 failed to occur in *rho1-2* cells (Fig. 8 B). In addition, *rho1-2* caused cells to arrest in mitosis, as revealed by a failure to degrade the mitotic cyclin Clb2 (Fig. 8 C). The arrest was dependent on Swe1. These observations are consistent with a role for Rho1 in signaling to Mih1 and Swe1. However, bud emergence and growth were delayed in *rho1-2* cells at the semirestrictive temperature. Thus, defects in mitotic events caused by *rho1-2* could be caused by defective signaling to Mih1 and Swe1 or to defects in bud growth.

To test for a role for Rho1 under conditions in which cell growth was not a complicating factor, we assayed the effects of a constitutively active form of Rho1 that was created by mutating glutamine 68 to histidine (referred to as Rho1*; Delley and Hall, 1999). Expression of *RHO1** from the *GAL1* promoter caused dephosphorylation of Mih1 in rapidly growing cells and in checkpoint-arrested cells (Fig. 8, D and E). Expression of *RHO1** failed to induce Mih1 dephosphorylation in cells carrying a temperature-sensitive allele of *PKC1* (*pkc1-21*; Fig. 8 D). Together, these data establish that Rho1 signals to Mih1 via Pkc1.

Rho1 is transported to the site of bud growth in association with secretory vesicles (McCaffrey et al., 1991; Abe et al., 2003; Forsmark et al., 2011). Rho1 associated with secretory vesicles is inactive; activation of Rho1 occurs at the site of membrane growth and is dependent on fusion of vesicles with the plasma membrane (Abe et al., 2003). A guanine nucleotide exchange factor that activates Rho1 is localized to the site of bud growth independent of membrane traffic (Abe et al., 2003). The fact

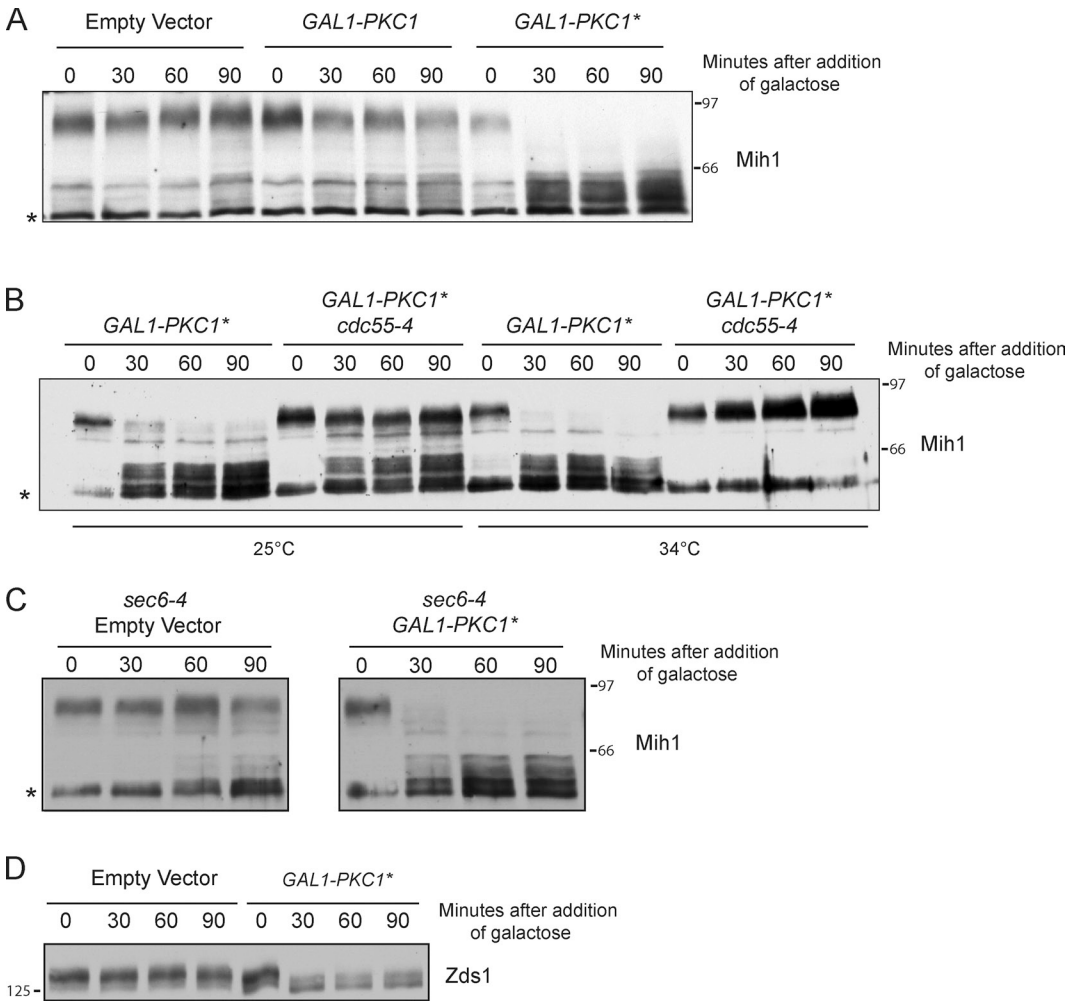

Figure 7. **Pkc1 signals to Mih1 via PP2A^{Cdc55}-Zds1/2.** (A) Cells were grown to log phase in YEP media containing 2% glycerol and 2% ethanol. Galactose was added, and cells were shifted to 30°C at t = 0. Mih1 phosphorylation was assayed by Western blotting. (B) Cells were grown to log phase in YEP media containing 2% glycerol and 2% ethanol. Galactose was added, and cells were shifted to 25 or 34°C at t = 0. Mih1 phosphorylation was assayed by Western blotting. (C) Cells were grown to log phase in YEP media containing 2% glycerol and 2% ethanol. Cells were shifted to 34°C for 60 min to induce a checkpoint arrest, and galactose was then added. Mih1 phosphorylation was assayed by Western blotting. (D) Cells were grown to log phase in YEP with 2% glycerol and 2% ethanol. Galactose was added, and cells were shifted to 30°C at t = 0. Zds1 phosphorylation was assayed by Western blotting. The asterisks denote background bands that appear with some batches of purified anti-Mih1 antibody. Numbers shown next to the Western blots indicate molecular mass in kilodaltons.

that activation of Rho1 is dependent on fusion of vesicles at the site of bud growth suggests a direct connection between membrane growth and signals that control Mih1 phosphorylation.

Signaling to Pkc1 may be proportional to the extent of polar bud growth

To further investigate the link between membrane traffic and mitosis, we explored the nature of the signals that control Pkc1. We raised an antibody against Pkc1 and used it to assay the behavior of Pkc1 during the cell cycle after release from a G1 arrest. We also assayed levels of a G1 cyclin (Cln2) and a mitotic cyclin (Clb2) in the same samples. Cln2/Cdk1 is required for initiation and maintenance of polar bud growth; Cln2 therefore provides a molecular marker for the period of polar bud growth (Cross, 1990; McCusker et al., 2007). Clb2/Cdk1 represses Cln2 transcription and induces the switch from polar growth to isotropic growth; Clb2 therefore provides a molecular marker for the switch from polar to isotropic bud growth and entry into mitosis (Amon et al., 1993; Lew and Reed, 1995b). The time course was performed at 22°C to slow down the cell cycle, which provided a better resolution of cell cycle events.

Pkc1 began to undergo hyperphosphorylation when Cln2 first appeared (Fig. 9 A). Interestingly, the peak of Pkc1 phosphorylation was reached at 80 min. At this point, Cln2 levels were declining, and Clb2 was beginning to accumulate, which corresponds to the switch from polar to isotropic bud growth. Thus, Pkc1 hyperphosphorylation was correlated with polar bud growth.

The fact that peak Pkc1 phosphorylation was not correlated with peak levels of Cln2 or Clb2 suggested that it is not controlled by direct signals from either of these cyclins. To determine whether Pkc1 phosphorylation is dependent on membrane traffic, we released wild-type and *sec6-4* cells from a G1 arrest

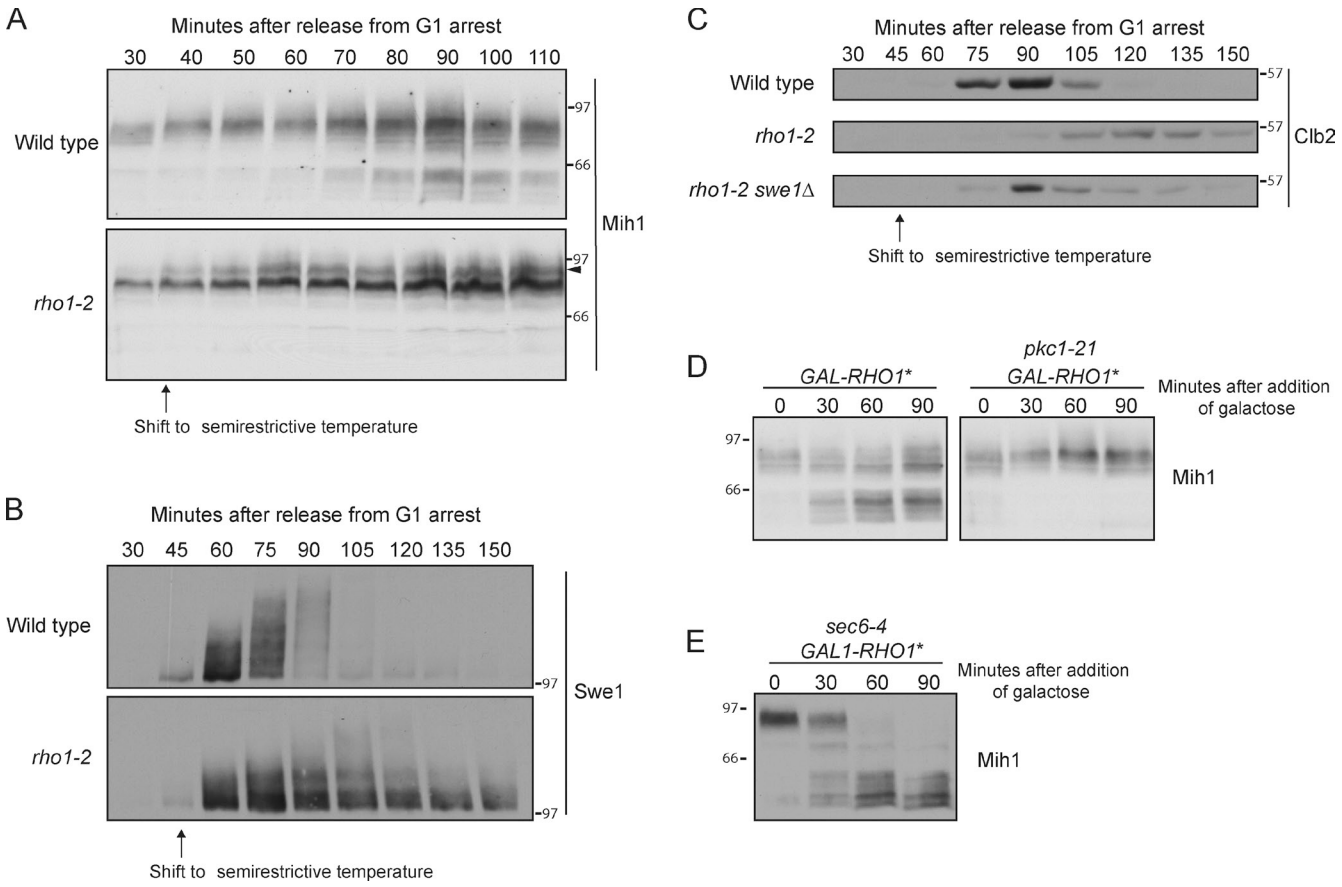

Figure 8. **Rho1 signals to Mih1 via Pkc1.** (A) Cells were released from a G1 arrest and shifted to a semirestrictive temperature (34°C) at 35 min after release. Mih1 phosphorylation was assayed by Western blotting. The arrowhead marks a hyperphosphorylated form that appears in the *rho1-2* cells. At 34°C, *rho1-2* cells grow slowly but are viable. (B) Cells were released from a G1 arrest and shifted to a semirestrictive temperature (34°C) at 45 min after release. Swe1 phosphorylation was assayed by Western blotting. (C) Cells were released from a G1 arrest and shifted to a semirestrictive temperature (34°C) at 45 min after release. Clb2 levels were assayed by Western blotting. (D) Cells were grown to log phase in YEP with 2% glycerol and 2% ethanol. Galactose was added, and the cells were shifted to 34°C at t = 0. Mih1 phosphorylation was assayed by Western blotting. The *pkc1-21* allele was used because it was found to cause rapid inactivation of Pkc1. (E) Cells were grown to log phase in YEP with 2% glycerol and 2% ethanol. The cells were shifted to 34°C for 60 min to induce a checkpoint arrest, and galactose was then added. Mih1 phosphorylation was assayed by Western blotting. Numbers shown next to the Western blots indicate molecular mass in kilodaltons.

and shifted them to the restrictive temperature at 70 min after release. Pkc1 phosphorylation was lost within 5 min, which is the same time scale observed for loss of Mih1 phosphorylation under these conditions (Figs. 3 and 9 B).

Discussion

A Rho1–Pkc1 signaling axis links membrane traffic to entry into mitosis

It has long been known that Wee1 and Cdc25 family members mediate a checkpoint that controls entry into mitosis, yet the cellular events that are monitored by the checkpoint have remained poorly understood. Here, we report that blocking membrane traffic causes a Swe1-dependent checkpoint arrest. The arrest is triggered via concerted effects on the regulation of both Swe1 and Mih1. $PP2A^{Cdc55}$ appears to be the agent of concerted checkpoint control. Signals regarding the status of membrane traffic are relayed to $PP2A^{Cdc55}$ via a signaling axis that includes Rho1, Pkc1, and Zds1/2. Fig. 10 A summarizes dependency relationships in the axis defined by loss- and gain-of-function mutants. Fig. 10 B summarizes known binding interactions (Kamada et al., 1996; Uetz et al., 2000; Drees et al., 2001; Queralt and Uhlmann, 2008; Yasutis et al., 2010; Wicky et al., 2011). Rho1, Pkc1, Zds1, and Cdc55 are all localized to the site of membrane growth, so they are well positioned to relay checkpoint signals (Yamochi et al., 1994; Andrews and Stark, 2000; Gentry and Hallberg, 2002; Rossio and Yoshida, 2011). It is not known whether they are found together in a single complex, as shown in the hypothetical model in Fig. 10 B, or whether they assemble as dynamic subcomplexes.

Signaling to Mih1 could be detected within minutes upon inactivation of Sec6. The rapidity of the response suggests that the checkpoint monitors membrane traffic events, rather than events that are disrupted as a secondary consequence of a block to membrane traffic. The Rho1–Pkc1 signaling axis suggests further connections to membrane traffic. Rho1 is transported on post-Golgi vesicles in an inactive form and becomes activated at the site of membrane growth (Abe et al., 2003). A mutant that blocks vesicle fusion at the site of growth also blocks Rho1 activation (Abe et al., 2003). In addition, Rom2, a guanine nucleotide exchange factor known to activate Rho1, is localized to the site of bud growth independently of membrane traffic

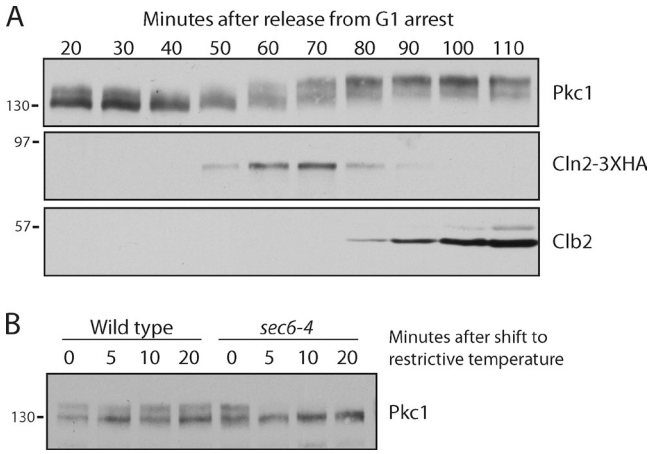

Figure 9. **Signaling to Pkc1 is dependent on membrane traffic.** (A) Cells were released from a G1 arrest at room temperature. The behavior of Pkc1, Cln2-3×HA, and Clb2 were assayed by Western blotting. All blots are from the same samples, so timing of events may be directly compared. (B) Wild-type and *sec6-4* cells were released from a G1 arrest. A sample was taken at 70 min (t = 0), and the cells were then shifted to the restrictive temperature (34°C). Pkc1 phosphorylation was assayed by Western blotting. Numbers shown next to the Western blots indicate molecular mass in kilodaltons.

(Abe et al., 2003). Active Rho1 directly binds Pkc1 and induces Pkc1 autophosphorylation, and Pkc1 undergoes hyperphosphorylation during the period of bud growth that is dependent on vesicle fusion. Pkc1, in turn, binds to $PP2A^{Cdc55}$-Zds1/2, which directly controls the phosphorylation states of Mih1 and Swe1 (Uetz et al., 2000; Drees et al., 2001; Pal et al., 2008; Yasutis et al., 2010; Wicky et al., 2011). Together, these observations connect Sec6-dependent vesicle fusion at the site of polar membrane growth to entry into mitosis.

A role for Rho1, Pkc1, and $PP2A^{Cdc55}$ in controlling entry into mitosis may be conserved. The closest human homologue of Pkc1 is called PRK2 (also called PKN2). PRK2 was found to control entry into mitosis, likely via regulation of Cdc25 (Schmidt et al., 2007). In *Drosophila melanogaster*, a close relative of Pkc1 controls proliferation and asymmetric division of neuroblasts and interacts with $PP2A^{Twins}$ (Chabu and Doe, 2009). Twins is the *Drosophila* homologue of Cdc55 and controls mitosis (Chen et al., 2007).

Previous genetic analysis suggested that the dephosphorylation of Mih1 is an important step in mechanisms required for activation of Mih1 during entry into mitosis (Pal et al., 2008; Wicky et al., 2011). The experiments reported here strengthen the link between Mih1 dephosphorylation and entry into mitosis, and they support a model in which hyperphosphorylation of Mih1 reflects the action of a checkpoint that keeps Mih1 inactive early in the cell cycle. It is not yet known whether hyperphosphorylation of Mih1 controls its localization or phosphatase activity. Thus far, it has not been possible to assay the activity of differently phosphorylated forms of Mih1 because it is a low abundance protein and shows poor solubility (unpublished data).

Disrupting membrane traffic caused cells to undergo a Swe1-dependent checkpoint arrest in early mitosis with low levels of mitotic cyclin. Interestingly, previous work has shown that inactivation of septins, or proteins that regulate the septins, causes a Swe1-dependent arrest or delay later in mitosis with high levels of mitotic cyclin (Carroll et al., 1998; Barral et al., 1999; Sreenivasan and Kellogg, 1999; Harvey et al., 2011). Together, these observations suggest that Swe1 may control multiple steps during entry into mitosis.

Key questions remain: How does phosphorylation control the activity or localization of Mih1? How does Pkc1 activate $PP2A^{Cdc55}$ to dephosphorylate Mih1? What is the functional significance of Zds1 phosphorylation? What are the kinases that phosphorylate Zds1? How do Zds1/2 target $PP2A^{Cdc55}$ to Mih1? These questions will be important directions for future analysis.

A growth-dependent signaling hypothesis for the G2-M checkpoint

Sec mutants block membrane traffic, which is essential for cell growth. Indeed, it is likely that the most ancient and conserved function of the secretory pathway is to generate membranes for cell growth. It is therefore tempting to speculate that the checkpoint monitors membrane growth to ensure that cell cycle progression is integrated with membrane growth. The checkpoint could also monitor membrane growth as part of a mechanism that controls cell size. Our observations, combined with previous observations, suggest interesting possibilities for how this could work. The fact that Rho1 is transported on vesicles and becomes activated at the site of membrane growth suggests a mechanism by which a signal could be generated that is dependent on and proportional to membrane growth: as more and more vesicles are delivered to the site of growth, the Rho1 signal could increase in strength (Fig. 10 C). Downstream components could read the signal and flip a switch when it reaches a threshold, thereby triggering cell cycle progression when sufficient growth has occurred. This model suggests that a cell size checkpoint could operate by monitoring the amount of growth that has occurred, rather than the absolute size of the cell. We refer to this as a growth-dependent signaling hypothesis for checkpoint function.

Interestingly, blocking membrane traffic causes rapid repression of ribosome biogenesis via Pkc1 (Li et al., 2000; Nanduri and Tartakoff, 2001). Thus, membrane traffic is linked to ribosome biogenesis. It is therefore conceivable that diverse aspects of cell growth and the cell cycle are regulated by signals generated via membrane growth.

There are several attractive features of a growth-dependent signaling hypothesis. A mechanism that monitors the extent of growth, rather than absolute cell size, would be adaptable to cells of diverse sizes and shapes. By linking signaling to the site of growth, the checkpoint could control the extent of growth at specific locations. In previous work, we found that the Swe1-dependent checkpoint specifically monitors the size or growth of the bud, which is consistent with the idea that the checkpoint can monitor growth at a specific site (Harvey and Kellogg, 2003). Growth-dependent signaling could also work in cells that do not increase their size via polar growth. In this case, growth at multiple sites over the surface of the cell could generate a signal that is read by downstream components. Another attractive

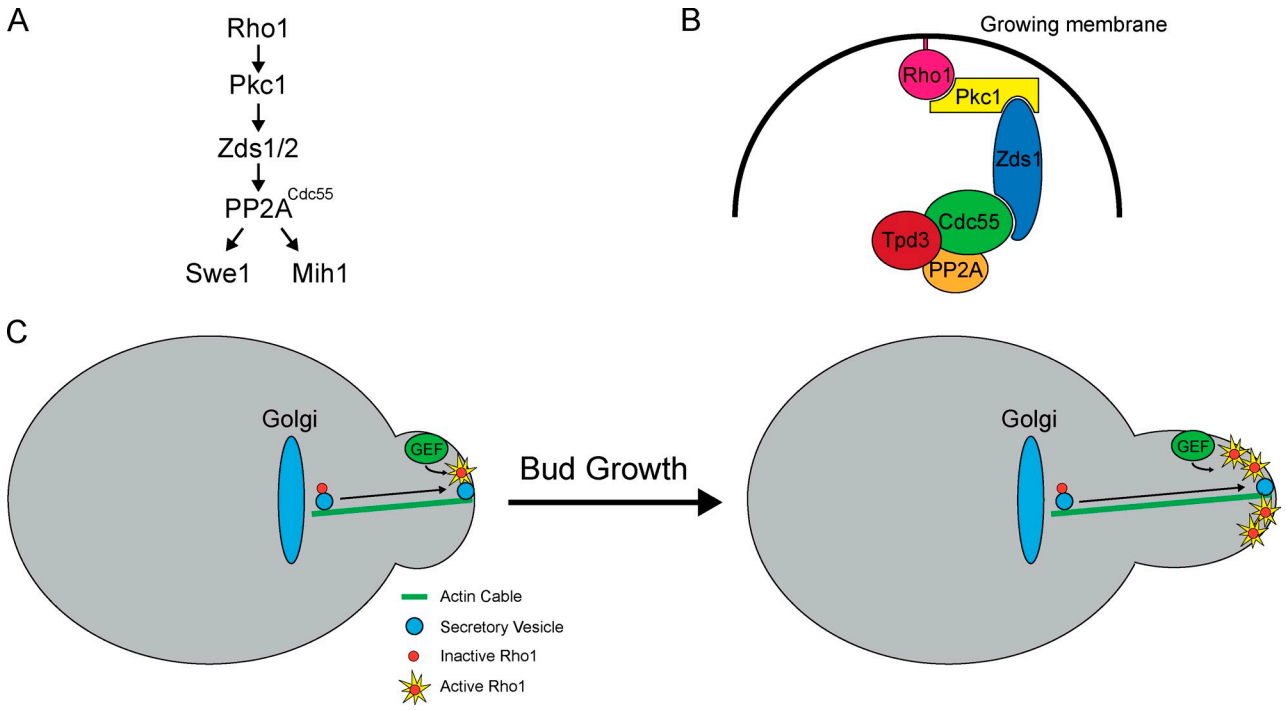

Figure 10. **A model for signals that link mitotic entry to membrane growth.** (A) Dependency relationships in the Rho1–Pkc1 signaling axis. (B) Known binding interactions in the Rho1–Pkc1 signaling axis. (C) A hypothetical model for generation of a signal that is proportional to membrane growth. Rho1 is activated at the site of membrane growth by a guanine nucleotide exchange factor (GEF). As more Rho1-bearing vesicles are delivered to the site of growth, the amount of active Rho1 increases. Downstream components of the signaling axis read the signal and flip a switch to initiate mitosis when the signal reaches a threshold level.

feature of growth-dependent signaling is that the proposed components are highly conserved and could carry out similar functions in all eukaryotic cells.

Although growth-dependent signaling is an appealing hypothesis, the data are currently consistent with alternative hypotheses. For example, the checkpoint may simply monitor whether membrane addition at the site of cell growth is occurring, rather than the extent of membrane growth. Another possibility is that the checkpoint monitors the concentration of active Rho1 or Pkc1 associated with the daughter bud membrane as a means of measuring absolute bud size. We also cannot yet rule out the possibility that blocking membrane traffic causes indirect effects on other cellular events that more directly trigger the checkpoint arrest.

Reconciling divergent views of the G2-M checkpoint

Pioneering work in fission yeast reached the conclusion that Wee1 and Cdc25 mediate a cell size checkpoint (Nurse, 1975). Subsequent studies found that budding yeast Swe1 and Mih1 are required for cell size control, which suggested the existence of a conserved cell size checkpoint (Russell et al., 1989; Jorgensen et al., 2002; Harvey and Kellogg, 2003; Pal et al., 2008). However, it has also been proposed that Swe1 and Mih1 mediate a checkpoint that monitors bud morphogenesis rather than size (Lew and Reed, 1995a; Lew, 2003; Keaton and Lew, 2006). The discovery that disrupting membrane traffic at the site of bud growth causes a checkpoint arrest suggests a way to reconcile these divergent views. Because localized membrane traffic is required for both cell growth and morphogenesis, the checkpoint could effectively monitor both events.

An appealing model is that the checkpoint controls the duration of polar growth by determining when the switch from polar to isotropic growth occurs. Because mitotic Cdk1 induces the switch, the timing of Cdk1 activation determines the timing of the switch. It is likely that the switch is induced early in mitosis by a low level of Cdk1 activity because G1 cyclins, which drive polar growth, begin to decline as soon as the mitotic cyclins appear (Fig. 9 A). Recent work defined a systems-level mechanism that generates and maintains low level Cdk1 activation in early mitosis (Deibler and Kirschner, 2010; Harvey et al., 2011). Interestingly, mathematical modeling suggests that low level activation of Mih1 is required for low level activation of Cdk1 (Harvey et al., 2011). Therefore, an interesting possibility is that hyperphosphorylation of Mih1 early in the cell cycle keeps it inactive. Pkc1-dependent dephosphorylation of Mih1 could then relieve inhibition of Mih1 and allow it to become active at a basal level that promotes low level activation of Cdk1/Clb2, thereby triggering the switch from polar to isotropic growth.

We found no evidence that expression of constitutively active Rho1 or Pkc1 from the GAL1 promoter could trigger destruction of Mcd1 or hyperphosphorylation of Swe1 in checkpoint-arrested cells. This may be an uninformative negative result. For example, overexpression of constitutively active Rho1 or Pkc1 may activate $PP2A^{Cdc55}$ to an artificially high level that blocks hyperphosphorylation of Swe1. Alternatively, the function of the Rho1–Pkc1 pathway may be to initiate early

Table 1. **Strains used in this study**

Strain	Genotype	Background	Reference
DK186	*MATa*	W303	Altman and Kellogg, 1997
DK177	*MATa BAR1*	W303	Altman and Kellogg, 1997
RSY2786	*MATa his3-Δ200 leu2-3,112 trp1-1 ura3-52 sec6-4 BAR1*	S288C	R. Schekman[a]
DK1440	*MATa sec6-4::His3MX6*	W303	This study
DK1473	*MATa his3-Δ200 leu2-3,112 trp1-1 ura3-52 sec6-4::kanMX6 BAR1*	S288C	This study
DK1475	*MATa sec6-4::kanMX6*	W303	This study
DK1606	*MATa sec6-4::kanMX6 cdc28Y19F-HA::URA3*	W303	This study
DK1600	*MATa sec6-4::kanMX6 swe1::His3MX6*	W303	This study
DK1731	*MATa MCD1-6×HA::natNT2*	W303	This study
DK1732	*MATa MCD1-6×HA::natNT2 sec6-4::kanMX6*	W303	This study
DK1733	*MATa MCD1-6×HA::natNT2 sec6-4::kanMX6 swe1::His3MX6*	W303	This study
DK936	*MATa sec7-4 his3-11 leu2-3/112 ura3-1*	S288C	A. Franzusoff
DK1496	*MATa cdc55-4::His3MX6 BAR1*	W303	Harvey et al., 2011
DK1631	*MATa PKC1::His3MX6*	W303	This study
DK1690	*MATa pkc1-14::His3MX6*	W303	This study
DK2095	*MATa pkc1-14::His3MX6 swe1::URA3*	W303	This study
DK1729	*MATa sec6-4::His3MX6 pDN3 [GAL1-RHO1-Q68H, URA3]*	W303	This study
DK1786	*MATa pDK20 [GAL1, URA3]*	W303	This study
DK1788	*MATa pSH32 [GAL1-3XHA, URA3]*	W303	This study
DK1790	*MATa pDN4A [GAL1-PKC1*-3×HA, URA3]*	W303	This study
DK1834	*MATa pDN5A [GAL1-PKC1-3×HA, URA3]*	W303	This study
DK1803	*MATa MCD1-6×HA::natNT2 sec6-4::kanMX6 pSH32 [GAL1-3×HA, URA3]*	W303	This study
DK1805	*MATa MCD1-6×HA::natNT2 sec6-4::kanMX6 pDN4A [GAL1-PKC1*-3×HA, URA3]*	W303	This study
DK1809	*MATa BAR1 pDN4A [GAL1-PKC1*-3×HA, URA3]*	W303	This study
DK1807	*MATa cdc55-4::His3MX6 pDN4A [GAL1-PKC1*-3×HA, URA3] BAR1*	W303	This study
DK1895	*MATa sec6-4::kanMX6 MCD1-6×HA::natNT2 pGAL1-ZDS1 [GAL1-ZDS1, URA3]*	W303	This study
SH761	*MATa cdc28-Y19F-HA::URA3*	W303	This study
HT195	*CDC55-3×HA::His3MX6*	W303	This study
DK354	*CDC55-3×HA::His3MX6 zds1Δ zds2Δ*	W303	Pal et al., 2008
DK1651	*pDN3 [GAL1-RHO1*, URA3]*	W303	This study
DK2084	*pkc1-21 pDN3 [GAL1-RHO1*, URA3]*	W303	This study
YPH499	*ura3 trp1 ade2 lys2 leu2 his3 gal-*	S288C	Saka et al., 2001
YOC772	*rho1Δ::HIS3 ade3::rho1-2::LEU2 ura3 trp1 ade2 lys2 leu2 his3 gal-*	S288C	Saka et al., 2001
DK1938	*pMT104 [CLN2-3×HA::LEU2]*	W303	This study

[a]University of California, Berkeley, Berkeley, CA.

mitotic events, including shutting off polar growth, without triggering full entry into mitosis.

A role for Wee1 and Cdc25 family members in determining the duration of polar growth could explain the paradoxical finding that loss of Wee1 causes a severe phenotype in fission yeast but only a mild phenotype in budding yeast. Fission yeast are completely dependent on polar growth. Thus, Wee1 mutants that disrupt the duration of polar growth should have severe consequences. In contrast, budding yeast have a short polar growth phase, which is followed by isotropic growth. Thus, loss of Swe1 would be expected to cause a mild decrease in cell size and formation of cells that are more round, which is the observed phenotype.

Cell growth, size, and shape are of fundamental importance, so it seems likely that they are controlled by conserved core mechanisms that appeared early in evolution. Wee1 and Cdc25 family members are highly conserved, yet a clear picture of their conserved functions in diverse cell types has remained surprisingly elusive. Further analysis of the signals that control Wee1 and Cdc25 family members is likely to lead to a more unified understanding of their functions in diverse cell types as well as a better understanding of the mysterious mechanisms that control cell growth, size, and shape.

Materials and methods

Yeast strains and culture conditions

The genotypes of the strains used in this study are listed in Table 1. All strains are in the W303-1A background (leu2-3,112 ura3-1 can1-100 ade2-1 his3-11,15 trp1-1 bar1Δ GAL+) except where noted. Cells were grown in YPD (yeast extract-peptone-dextrose) media supplemented with 40 mg/liter adenine, except where noted. To facilitate moving the *sec6-4* mutant allele into different strain backgrounds, the kanMX6 marker cassette was integrated 256 base pairs downstream of the *sec6-4* allele in strain RSY2786 to create strain DK1473 (oligonucleotides [oligos] 5′-CGAAACTTTCTCTTCCGAAAAAATTTCCAGGCAGTATTCCCGCGGATCCCCGGGTTAATTAA-3′ and 5′-GCTCCGTCTAGAGAATGACACGAAACCTCACTCGTTGTTTCCGAATTCGAGCTCGTTTAAAC-3′). To transfer the *sec6-4* mutant allele into different strain backgrounds, PCR was used to amplify *sec6-4* along with the KanMX6 cassette and flanking DNA, and the resulting product was used to transform cells (oligos 5′-CCACCACATTGGAACATATTTGAAGTATAC-3′ and 5′-CATTGCTACCAAGCTAACAAAAGGATCAGG-3′). Transformants were selected on G418 and screened for temperature sensitivity to identify which ones recombined the *sec6-4*

allele into the genome. This approach was used to put the *sec6-4* allele in strains DK186 and SH761, thereby creating strains DK1475 and DK1606, respectively. Strain DK936 was generated by switching the mating type of strain AFY39 to *MATa* (Deitz et al., 2000). Strains DK1731, DK1732, and DK1733 were generated by putting a 6×HA tag at the C terminus of *MCD1* in DK186, DK1475, and DK1600 using a PCR-based approach (oligos 5′-ATAGACGCCAAACCTGCACTATTTGAAAGGTTTATCAATGCTCGTAC-GCTGCAGGTCGAC-3′ and 5′-TTGGGTCCACCAAGAAATCCCCTCG-GCGTAACTAGGTTTTAATCGATGAATTCGAGCTCG-3′; Janke et al., 2004). Strain DK1895 was generated by digesting plasmid pGAL-ZDS1 with NcoI to target integration at the URA3 locus in strain DK1732. Strain DK1729 was created by digesting pDN3 with StuI to target integration at the *URA3* locus in strain DK1440. Strains DK1725 and DK1786 were created by digesting pDK20 with StuI to target integration at the *URA3* locus in strains DK1440 and DK186. Strain DK1788 was created by digesting pSH32 with ApaI to target integration at the *URA3* locus in strain DK186. Strains DK1790, DK1807, and DK1809 were created by digesting pDN4A with ApaI to target integration at the *URA3* locus in strains DK186, DK1496, and DK177. Strain DK1834 was created by digesting pDN5A with ApaI to target integration at the *URA3* locus in strain DK186.

Plasmid construction and generation of anti-Pkc1 antibodies

An integrating plasmid that expresses *ZDS1* from the *GAL1* promoter was created by amplifying the *ZDS1* open reading frame by PCR and cloning into the EcoR1 and BamH1 sites of pDK20 to create pGAL1-ZDS1 (oligos 5′-GCGGAATTCATGTCCAATAGAGATAACGAGAGC-3′ and 5′-GCGGGATCCTCAGGGTTGTTGTTGTTGTTG-3′). This plasmid can be cut with Nco1 to target integration at *URA3*. An integrating vector that expresses *RHO1* from the *GAL1* promoter was created by amplifying the *RHO1* open reading frame and cloning into the HindIII and EagI sites of pDK20 to create pDN1 (oligos 5′-GCGCAAGCTTATGTCACAACAAGTT-GGTAACAGTATCAGAAGA-3′ and 5′-CGCCGGCCGCTATAACAAGA-CACACTTCTTCTTCTTCTTTTCAGTAGT-3′). This plasmid can be cut with Stu1 to target integration at *URA3*. To create a plasmid that expresses constitutively active *RHO1* (*RHO1**) from the *GAL1* promoter, site-directed mutagenesis was used to convert glutamine 68 to histidine in pDN1 to create pDN3 (oligos 5′-TGGGATACCGCTGGTCACGAAGATTATGATAGA-3′ and 5′-TCTATCATAATCTTCGTGACCAGCGGTATCCCA-3′; Delley and Hall, 1999). An integrating plasmid that expresses constitutively active *PKC1* (*PKC1**) tagged with 3×HA was created by amplifying *PKC1** from pGAL1-PKC1* (Delley and Hall, 1999) and cloning into the Eag1 and Xho1 sites of pSH32 to create pDN4A (oligos 5′-GCGCTCGAGATGAGTTTTTC-ACAATTGGAGCAGAACATTAAAAAAAAGA-3′ and 5′-GGAAGTGA-CGGCCGTAAATCCAAATCATCTGGCATAAAGGAAAATCCTCTAAAC-3′). An integrating plasmid that expresses wild-type *PKC1* from the *GAL1* promoter was created by mutagenizing *PKC1** in pDN4A back to wild type to create pDN5A (oligos 5′-GCAGTTGATGGGTGGACTACATCGT-CATGGTGCTATTATCAATAGG-3′ and 5′-CCTATTGATAATAGCACCAT-GACGATGTAGTCCACCCATCAACTGC-3′). To make an antibody that recognizes Pkc1, the N terminus of *PKC1* was amplified and recombined into the vector pDONR221 (Gateway; Invitrogen) to create pDK117 (oligos 5′-GAAAACCTGTACTTCCAGTCCATGAGTTTTTCACAATTGGAGCA-GAAC-3′ and 5′-GTCAAGAAAGCTGGGTCTCACGGTTGTTGATTATC-CATTATGTCATT-3′). The N terminus was then recombined into pDEST15 to create pDK118, which allows expression as a GST fusion. The GST-Pkc1 fusion was purified and used to immunize a rabbit using standard protocols. The serum was run over a GST column to deplete anti-GST antibodies and was then run over a GST-Pkc1 column to purify anti-Pkc1 antibodies. To test the specificity of the antibody, we probed extracts from wild-type cells and from cells in which Pkc1 was fused to CFP. The Pkc1-CFP fusion was shifted above untagged Pkc1, which revealed that there are no background bands in the vicinity of Pkc1 (Fig. S1). Cells carrying the Pkc1-CFP fusion protein as their sole source of Pkc1 grew slowly at low temperatures and were nearly inviable at 37°C, which indicated that the protein was not fully functional. This could explain why multiple phosphorylation forms of the Pkc1-GFP fusion protein were not observed.

Cell cycle time courses

Cells were grown overnight at room temperature to an OD_{600} of 0.65 and were then arrested in G1 by the addition of α-factor to either 0.5 µg/ml (for *bar1Δ* strains) or 15 µg/ml (for *BAR1* strains) for 3 h. Cells were released from the arrest by washing 3× with fresh YPD media at room temperature. For time courses involving a temperature shift, cultures were incubated at room temperature before the shift and were transferred to a shaking water bath to shift the temperature. For expression of galactose-inducible promoters, cells were grown overnight in YEP (yeast extract peptone) containing 2% raffinose or 2% glycerol and 2% ethanol. Expression was initiated by addition of galactose to 2%.

At each time point, 1.6-ml samples were collected in screw-cap tubes. The cells were rapidly pelleted, the supernatant was removed, and 250 µl of glass beads was added before freezing on liquid nitrogen. To lyse cells, 140 µl of sample buffer (65 mM Tris-HCl, pH 6.8, 3% SDS, 10% glycerol, 5% β-mercaptoethanol, 50 mM NaF, and 100 mM β-glycerophosphate) was added. 2 mM PMSF was added to the sample buffer immediately before use from a 100-mM stock made in 100% ethanol. To lyse cells, tubes were placed in a disrupter (Multibeater-8; BioSpec) at top speed for 2 min. The tubes were immediately removed, centrifuged for 13 s in a microfuge (5415C; Eppendorf), and then placed in a boiling water bath for 5 min. After boiling, the tubes were centrifuged again for 5 min, and either 5 µl (for Zds1) or 20 µl was loaded on a gel. To assay nuclear division, 250-µl samples were collected, and the cells were pelleted and fixed by resuspending in 250 µl of 70% ethanol and 30% 50 mM Tris-HCl, pH 8.0. Nuclei were stained with Sytox green, and the presence of multiple nuclei was assayed by microscopy. To assay mitotic spindle assembly, cells were fixed with formaldehyde and stained with antitubulin as previously described (Harvey and Kellogg, 2003). At each time point, a minimum of 200 cells was scored for the presence of short or long spindles.

Western blotting

PAGE and Western blotting were performed as previously described (Anderson et al., 1973; Harvey et al., 2011). All gels were run at 20 mA on the constant current setting. For Mih1 and HA Western blots, electrophoresis was performed on a 10% polyacrylamide gel until a 29-kD prestained marker ran to the bottom of the gel. For Swe1 Western blots, electrophoresis was performed on a 10% polyacrylamide gel until a 66.5-kD marker ran to the bottom of the gel. For Zds1 Western blots, electrophoresis was performed on a 9% polyacrylamide gel until a 65-kD marker ran to the bottom of the gel. For Pkc1 Western blots, electrophoresis was performed on a 9% polyacrylamide gel until a 57.6-kD marker ran to the bottom of the gel. Western blots were transferred for 90 min at 800 mA at 4°C in a transfer tank (Hoeffer) in a buffer containing 20 mM Tris base, 150 mM glycine, and 20% methanol. Blots were probed overnight at 4°C with affinity-purified rabbit polyclonal antibodies raised against a Mih1, Swe1, Zds1, Pkc1, or HA peptide. Blots were probed with an HRP-conjugated donkey anti–rabbit secondary antibody (GE Healthcare).

Coimmunoprecipitation

Coimmunoprecipitation of Pkc1 and $PP2A^{Cdc55}$-Zds1/2 was assayed as previously described with the following modifications (Mortensen et al., 2002). Strains DK186 (untagged control), HT195 (*CDC55-3×HA*), and DK354 (*CDC55-3×HA zds1Δ zds2Δ*) were grown to an OD of 0.7 in YPD media at room temperature. Cells from 50 ml of each cell culture were pelleted, resuspended in 1 ml YPD, pelleted again in a 2-ml tube, and frozen on liquid nitrogen.

Immunoaffinity beads were made by binding mouse anti-HA monoclonal antibodies (Santa Cruz Biotechnology, Inc.) to protein A beads (Bio-Rad Laboratories) overnight at 4°C on a rotator (Labquake Rotisserie; Barnstead Thermolyne). For each immunoprecipitation, 10 µg anti-HA antibody was bound to 15 µl protein A beads in the presence of phosphate-buffered saline containing 500 mM NaCl and 0.1% Tween 20.

Cell extracts were made by adding 300 µl of acid-washed glass beads to frozen cell pellets followed by 300 µl of cold lysis buffer (50 mM Hepes-KOH, pH 7.6, 75 mM B glycerol phosphate, 50 mM NaF, 1 mM $MgCl_2$, 1 mM EGTA, 5% glycerol, 0.25% Tween 20, and 1 mM PMSF). The tubes were immediately placed into a disrupter (Multibeater-8) and shaken at top speed for 25 s. The tubes were briefly spun at 14,000 rpm in a microfuge to collect the sample at the bottom of the tube and then placed in an ice-water bath for 5 min. 250 µl supernatant was transferred to a new 1.5-ml tube and replaced with 250 µl lysis buffer. The tubes were beaten again for 25 s. 250 µl supernatant was removed, pooled with the first supernatant, centrifuged at 14,000 rpm in a microfuge for 10 min at 4°C, and then added to the immunoaffinity beads equilibrated in lysis buffer. A 10-µl sample of the extract was taken before treatment with antibody and frozen in liquid nitrogen for analysis by Western blotting. The tubes were rotated gently end over end at 4°C for 1 h and 45 min and then washed three times batchwise with 400 µl lysis buffer without PMSF. Cdc55-3×HA and associated proteins were eluted from the beads by the addition of 150 µl elution buffer (50 mM Hepes-KOH, pH 7.6, 1 M NaCl, 1 mM $MgCl_2$, 1 mM EGTA, 5% glycerol, and 0.5 mg/ml HA dipeptide) at room temperature. The beads were incubated for 15 min and gently mixed every few minutes to allow for mixing of the beads. The beads were pelleted in a microfuge, and 125 µl of the supernatant was removed, taking

care to avoid the antibody-containing beads. This process was repeated once more with the exception that 150 µl of the supernatant was removed. The supernatants were pooled and precipitated by the addition of trichloroacetic acid to 10%. The resulting pellet was resuspended in 25 µl protein sample buffer; 20 and 2 µl were loaded onto a 9% polyacrylamide gel and used for a Western blot probing for Pkc1 and Cdc55-3×HA, respectively. For Western blotting of the crude extracts, 90 µl protein sample buffer was added to 10 µl of crude extract, the samples were boiled, and 15 µl was loaded onto an SDS-PAGE gel.

Generation of temperature-sensitive alleles of PKC1

To generate a collection of *PKC1* temperature-sensitive alleles, we first used a PCR-based approach to integrate the His3MX6 marker cassette downstream of the *PKC1* gene in the wild-type strain DK186, creating strain DK1631 (oligos 5′-GCCGTATGTTCAACAATGCGCATTCTGTTTACATTATTAACGGATCCCCGGGTTAATTAA-3′ and 5′-CTGTCAACTTTAGAAATATGTTAGTAGTAATATAATCCTGAGCGAATTCGAGCTCGTTTAAC-3′). Genomic DNA was purified from this strain and used as a template to amplify the PKC1-His3MX6 fragment and flanking DNA by PCR using *Pfu* polymerase (oligos 5′-GCTATTCAATTTGGCTGAGTAG-3′ and 5′-GCTTTGAGTATAGTCGAATGTG-3′). The PCR product was gel purified and used as a template to carry out a large-scale PCR reaction with the error-prone *Taq* polymerase (oligos 5′-GATAGCCGTCGAAGAAAATA-3′ and 5′-GATTCGTCCATTTATGCCGTAT-3′). The PCR reaction was then transformed into DK186 and plated onto –His plates at ∼150 colonies per plate to screen ∼4,500 colonies for temperature sensitivity by replica plating. To eliminate mutants in the HIS gene, candidates were also tested for temperature sensitivity on YPD plates, and mutants were further tested for rescue by wild-type *PKC1* on a centromere plasmid. The screen identified 36 temperature-sensitive alleles of *PKC1*. To screen the collection for defects in cell growth, mutants were struck on YPD plates and left to grow at room temperature, 34, or 37°C for 2 d. Cell morphology was examined by light microscopy.

Microscopy

Yeast cells were fixed with formaldehyde and photographed using a microscope (Axioskop; Carl Zeiss) fitted with a 100× Plan-Neofluar 1.3 NA objective and a camera (AxioCam HRm; Carl Zeiss). Images were acquired using AxioVision software (Carl Zeiss). Actin was stained with FITC-phalloidin.

Latrunculin A treatment

For Fig. 4, cells were released from an α-factor arrest into fresh YPD media at room temperature. After 70 min, the presence of small buds was verified by microscopy. The culture was then split in half, and latrunculin A was added to a final concentration of 100 µM to one half of the culture, whereas an equal volume of DMSO was added to the other half.

Online supplemental material

Fig. S1 shows the specificity of the anti-Pkc1 antibody. Online supplemental material is available at http://www.jcb.org/cgi/content/full/jcb.201108108/DC1.

We thank members of the laboratory and Needhi Bhalla for helpful advice and critical reading of the manuscript.

This work was supported by the University of California Cancer Research Coordinating Committee and the National Institutes of Health (grant GM069602). V. Thai was supported by a National Institutes of Health Postdoctoral Fellowship (grant F32GM087103-02).

Submitted: 18 August 2011
Accepted: 23 February 2012

References

Abe, M., H. Qadota, A. Hirata, and Y. Ohya. 2003. Lack of GTP-bound Rho1p in secretory vesicles of *Saccharomyces cerevisiae*. *J. Cell Biol.* 162:85–97. http://dx.doi.org/10.1083/jcb.200301022

Altman, R., and D.R. Kellogg. 1997. Control of mitotic events by Nap1 and the Gin4 kinase. *J. Cell Biol.* 138:119–130. http://dx.doi.org/10.1083/jcb.138.1.119

Amon, A., M. Tyers, B. Futcher, and K. Nasmyth. 1993. Mechanisms that help the yeast cell cycle clock tick: G2 cyclins transcriptionally activate G2 cyclins and repress G1 cyclins. *Cell*. 74:993–1007. http://dx.doi.org/10.1016/0092-8674(93)90722-3

Amon, A., S. Irniger, and K. Nasmyth. 1994. Closing the cell cycle circle in yeast: G2 cyclin proteolysis initiated at mitosis persists until the activation of G1 cyclins in the next cycle. *Cell*. 77:1037–1050. http://dx.doi.org/10.1016/0092-8674(94)90443-X

Anderson, C.W., P.R. Baum, and R.F. Gesteland. 1973. Processing of adenovirus 2-induced proteins. *J. Virol.* 12:241–252.

Andrews, P.D., and M.J. Stark. 2000. Dynamic, Rho1p-dependent localization of Pkc1p to sites of polarized growth. *J. Cell Sci.* 113:2685–2693.

Asano, S., J.E. Park, K. Sakchaisri, L.R. Yu, S. Song, P. Supavilai, T.D. Veenstra, and K.S. Lee. 2005. Concerted mechanism of Swe1/Wee1 regulation by multiple kinases in budding yeast. *EMBO J.* 24:2194–2204. http://dx.doi.org/10.1038/sj.emboj.7600683

Babu, P., J.D. Bryan, H.R. Panek, S.L. Jordan, B.M. Forbrich, S.C. Kelley, R.T. Colvin, and L.C. Robinson. 2002. Plasma membrane localization of the Yck2p yeast casein kinase 1 isoform requires the C-terminal extension and secretory pathway function. *J. Cell Sci.* 115:4957–4968. http://dx.doi.org/10.1242/jcs.00203

Balasubramanian, M.K., D. McCollum, and U. Surana. 2000. Tying the knot: linking cytokinesis to the nuclear cycle. *J. Cell Sci.* 113:1503–1513.

Barral, Y., M. Parra, S. Bidlingmaier, and M. Snyder. 1999. Nim1-related kinases coordinate cell cycle progression with the organization of the peripheral cytoskeleton in yeast. *Genes Dev.* 13:176–187. http://dx.doi.org/10.1101/gad.13.2.176

Booher, R.N., R.J. Deshaies, and M.W. Kirschner. 1993. Properties of *Saccharomyces cerevisiae* wee1 and its differential regulation of $p34^{CDC28}$ in response to G1 and G2 cyclins. *EMBO J.* 12:3417–3426.

Carroll, C.W., R. Altman, D. Schieltz, J.R. Yates, and D.R. Kellogg. 1998. The septins are required for the mitosis-specific activation of the Gin4 kinase. *J. Cell Biol.* 143:709–717. http://dx.doi.org/10.1083/jcb.143.3.709

Chabu, C., and C.Q. Doe. 2009. Twins/PP2A regulates aPKC to control neuroblast cell polarity and self-renewal. *Dev. Biol.* 330:399–405. http://dx.doi.org/10.1016/j.ydbio.2009.04.014

Chen, F., V. Archambault, A. Kar, P. Lio', P.P. D'Avino, R. Sinka, K. Lilley, E.D. Laue, P. Deak, L. Capalbo, and D.M. Glover. 2007. Multiple protein phosphatases are required for mitosis in *Drosophila*. *Curr. Biol.* 17:293–303. http://dx.doi.org/10.1016/j.cub.2007.01.068

Coleman, T.R., Z. Tang, and W.G. Dunphy. 1993. Negative regulation of the wee1 protein kinase by direct action of the nim1/cdr1 mitotic inducer. *Cell*. 72:919–929. http://dx.doi.org/10.1016/0092-8674(93)90580-J

Cross, F.R. 1990. Cell cycle arrest caused by CLN gene deficiency in *Saccharomyces cerevisiae* resembles START-I arrest and is independent of the mating-pheromone signalling pathway. *Mol. Cell. Biol.* 10:6482–6490.

Deibler, R.W., and M.W. Kirschner. 2010. Quantitative reconstitution of mitotic CDK1 activation in somatic cell extracts. *Mol. Cell*. 37:753–767. http://dx.doi.org/10.1016/j.molcel.2010.02.023

Deitz, S.B., A. Rambourg, F. Képès, and A. Franzusoff. 2000. Sec7p directs the transitions required for yeast Golgi biogenesis. *Traffic*. 1:172–183. http://dx.doi.org/10.1034/j.1600-0854.2000.010209.x

Delley, P.A., and M.N. Hall. 1999. Cell wall stress depolarizes cell growth via hyperactivation of RHO1. *J. Cell Biol.* 147:163–174. http://dx.doi.org/10.1083/jcb.147.1.163

Drees, B.L., B. Sundin, E. Brazeau, J.P. Caviston, G.C. Chen, W. Guo, K.G. Kozminski, M.W. Lau, J.J. Moskow, A. Tong, et al. 2001. A protein interaction map for cell polarity development. *J. Cell Biol.* 154:549–571. http://dx.doi.org/10.1083/jcb.200104057

Dunphy, W.G., and A. Kumagai. 1991. The cdc25 protein contains an intrinsic phosphatase activity. *Cell*. 67:189–196. http://dx.doi.org/10.1016/0092-8674(91)90582-J

Finger, F.P., and P. Novick. 1997. Sec3p is involved in secretion and morphogenesis in *Saccharomyces cerevisiae*. *Mol. Biol. Cell*. 8:647–662.

Forsmark, A., G. Rossi, I. Wadskog, P. Brennwald, J. Warringer, and L. Adler. 2011. Quantitative proteomics of yeast post-Golgi vesicles reveals a discriminating role for Sro7p in protein secretion. *Traffic*. 12:740–753. http://dx.doi.org/10.1111/j.1600-0854.2011.01186.x

Gachet, Y., S. Tournier, J.B. Millar, and J.S. Hyams. 2001. A MAP kinase-dependent actin checkpoint ensures proper spindle orientation in fission yeast. *Nature*. 412:352–355. http://dx.doi.org/10.1038/35085604

Gautier, J., M.J. Solomon, R.N. Booher, J.F. Bazan, and M.W. Kirschner. 1991. cdc25 is a specific tyrosine phosphatase that directly activates p34cdc2. *Cell*. 67:197–211. http://dx.doi.org/10.1016/0092-8674(91)90583-K

Gentry, M.S., and R.L. Hallberg. 2002. Localization of *Saccharomyces cerevisiae* protein phosphatase 2A subunits throughout mitotic cell cycle. *Mol. Biol. Cell*. 13:3477–3492. http://dx.doi.org/10.1091/mbc.02-05-0065

Gould, K.L., and P. Nurse. 1989. Tyrosine phosphorylation of the fission yeast $cdc2^{+}$ protein kinase regulates entry into mitosis. *Nature*. 342:39–45. http://dx.doi.org/10.1038/342039a0

Harvey, S.L., and D.R. Kellogg. 2003. Conservation of mechanisms controlling entry into mitosis: budding yeast wee1 delays entry into mitosis and is required for cell size control. *Curr. Biol.* 13:264–275. http://dx.doi.org/10.1016/S0960-9822(03)00049-6

Harvey, S.L., A. Charlet, W. Haas, S.P. Gygi, and D.R. Kellogg. 2005. Cdk1-dependent regulation of the mitotic inhibitor Wee1. *Cell*. 122:407–420. http://dx.doi.org/10.1016/j.cell.2005.05.029

Harvey, S.L., G. Enciso, N.E. Dephoure, S.P. Gygi, J. Gunawardena, and D.R. Kellogg. 2011. A phosphatase threshold sets the level of Cdk1 activity in early mitosis in budding yeast. *Mol. Biol. Cell*. 22:3595–3608. http://dx.doi.org/10.1091/mbc.E11-04-0340

Izumi, T., and J.L. Maller. 1993. Elimination of cdc2 phosphorylation sites in the cdc25 phosphatase blocks initiation of M-phase. *Mol. Biol. Cell*. 4:1337–1350.

Janke, C., M.M. Magiera, N. Rathfelder, C. Taxis, S. Reber, H. Maekawa, A. Moreno-Borchart, G. Doenges, E. Schwob, E. Schiebel, and M. Knop. 2004. A versatile toolbox for PCR-based tagging of yeast genes: new fluorescent proteins, more markers and promoter substitution cassettes. *Yeast*. 21:947–962. http://dx.doi.org/10.1002/yea.1142

Jorgensen, P., and M. Tyers. 2004. How cells coordinate growth and division. *Curr. Biol.* 14:R1014–R1027. http://dx.doi.org/10.1016/j.cub.2004.11.027

Jorgensen, P., J.L. Nishikawa, B.J. Breitkreutz, and M. Tyers. 2002. Systematic identification of pathways that couple cell growth and division in yeast. *Science*. 297:395–400. http://dx.doi.org/10.1126/science.1070850

Kamada, Y., H. Qadota, C.P. Python, Y. Anraku, Y. Ohya, and D.E. Levin. 1996. Activation of yeast protein kinase C by Rho1 GTPase. *J. Biol. Chem.* 271:9193–9196. http://dx.doi.org/10.1074/jbc.271.16.9193

Karpova, T.S., S.L. Reck-Peterson, N.B. Elkind, M.S. Mooseker, P.J. Novick, and J.A. Cooper. 2000. Role of actin and Myo2p in polarized secretion and growth of *Saccharomyces cerevisiae*. *Mol. Biol. Cell*. 11:1727–1737.

Keaton, M.A., and D.J. Lew. 2006. Eavesdropping on the cytoskeleton: progress and controversy in the yeast morphogenesis checkpoint. *Curr. Opin. Microbiol.* 9:540–546. http://dx.doi.org/10.1016/j.mib.2006.10.004

Kellogg, D.R. 2003. Wee1-dependent mechanisms required for coordination of cell growth and cell division. *J. Cell Sci.* 116:4883–4890. http://dx.doi.org/10.1242/jcs.00908

Kumagai, A., and W.G. Dunphy. 1991. The cdc25 protein controls tyrosine dephosphorylation of the cdc2 protein in a cell-free system. *Cell*. 64:903–914. http://dx.doi.org/10.1016/0092-8674(91)90315-P

Kumagai, A., and W.G. Dunphy. 1992. Regulation of the cdc25 protein during the cell cycle in *Xenopus* extracts. *Cell*. 70:139–151. http://dx.doi.org/10.1016/0092-8674(92)90540-S

Levin, D.E., and E. Bartlett-Heubusch. 1992. Mutants in the *S. cerevisiae* PKC1 gene display a cell cycle–specific osmotic stability defect. *J. Cell Biol.* 116:1221–1229. http://dx.doi.org/10.1083/jcb.116.5.1221

Lew, D.J. 2003. The morphogenesis checkpoint: how yeast cells watch their figures. *Curr. Opin. Cell Biol.* 15:648–653. http://dx.doi.org/10.1016/j.ceb.2003.09.001

Lew, D.J., and S.I. Reed. 1993. Morphogenesis in the yeast cell cycle: regulation by Cdc28 and cyclins. *J. Cell Biol.* 120:1305–1320. http://dx.doi.org/10.1083/jcb.120.6.1305

Lew, D.J., and S.I. Reed. 1995a. A cell cycle checkpoint monitors cell morphogenesis in budding yeast. *J. Cell Biol.* 129:739–749. http://dx.doi.org/10.1083/jcb.129.3.739

Lew, D.J., and S.I. Reed. 1995b. Cell cycle control of morphogenesis in budding yeast. *Curr. Opin. Genet. Dev.* 5:17–23. http://dx.doi.org/10.1016/S0959-437X(95)90048-9

Li, Y., R.D. Moir, I.K. Sethy-Coraci, J.R. Warner, and I.M. Willis. 2000. Repression of ribosome and tRNA synthesis in secretion-defective cells is signaled by a novel branch of the cell integrity pathway. *Mol. Cell. Biol.* 20:3843–3851. http://dx.doi.org/10.1128/MCB.20.11.3843-3851.2000

Lim, H.H., P.Y. Goh, and U. Surana. 1996. Spindle pole body separation in *Saccharomyces cerevisiae* requires dephosphorylation of the tyrosine 19 residue of Cdc28. *Mol. Cell. Biol.* 16:6385–6397.

Lin, F.C., and K.T. Arndt. 1995. The role of *Saccharomyces cerevisiae* type 2A phosphatase in the actin cytoskeleton and in entry into mitosis. *EMBO J.* 14:2745–2759.

Ma, X.J., Q. Lu, and M. Grunstein. 1996. A search for proteins that interact genetically with histone H3 and H4 amino termini uncovers novel regulators of the Swe1 kinase in *Saccharomyces cerevisiae*. *Genes Dev.* 10:1327–1340. http://dx.doi.org/10.1101/gad.10.11.1327

McCaffrey, M., J.S. Johnson, B. Goud, A.M. Myers, J. Rossier, M.R. Popoff, P. Madaule, and P. Boquet. 1991. The small GTP-binding protein Rho1p is localized on the Golgi apparatus and post-Golgi vesicles in *Saccharomyces cerevisiae*. *J. Cell Biol.* 115:309–319. http://dx.doi.org/10.1083/jcb.115.2.309

McCusker, D., C. Denison, S. Anderson, T.A. Egelhofer, J.R. Yates III, S.P. Gygi, and D.R. Kellogg. 2007. Cdk1 coordinates cell-surface growth with the cell cycle. *Nat. Cell Biol.* 9:506–515. http://dx.doi.org/10.1038/ncb1568

McNulty, J.J., and D.J. Lew. 2005. Swe1p responds to cytoskeletal perturbation, not bud size, in *S. cerevisiae*. *Curr. Biol.* 15:2190–2198. http://dx.doi.org/10.1016/j.cub.2005.11.039

Minshull, J., A. Straight, A.D. Rudner, A.F. Dernburg, A. Belmont, and A.W. Murray. 1996. Protein phosphatase 2A regulates MPF activity and sister chromatid cohesion in budding yeast. *Curr. Biol.* 6:1609–1620. http://dx.doi.org/10.1016/S0960-9822(02)70784-7

Mortensen, E.M., H. McDonald, J. Yates III, and D.R. Kellogg. 2002. Cell cycle-dependent assembly of a Gin4-septin complex. *Mol. Biol. Cell*. 13:2091–2105. http://dx.doi.org/10.1091/mbc.01-10-0500

Mueller, P.R., T.R. Coleman, and W.G. Dunphy. 1995. Cell cycle regulation of a *Xenopus* Wee1-like kinase. *Mol. Biol. Cell*. 6:119–134.

Mulholland, J., A. Wesp, H. Riezman, and D. Botstein. 1997. Yeast actin cytoskeleton mutants accumulate a new class of Golgi-derived secretary vesicle. *Mol. Biol. Cell*. 8:1481–1499.

Nanduri, J., and A.M. Tartakoff. 2001. The arrest of secretion response in yeast: signaling from the secretory path to the nucleus via Wsc proteins and Pkc1p. *Mol. Cell*. 8:281–289. http://dx.doi.org/10.1016/S1097-2765(01)00312-4

Nurse, P. 1975. Genetic control of cell size at cell division in yeast. *Nature*. 256:547–551. http://dx.doi.org/10.1038/256547a0

Nurse, P., P. Thuriaux, and K. Nasmyth. 1976. Genetic control of the cell division cycle in the fission yeast *Schizosaccharomyces pombe*. *Mol. Gen. Genet.* 146:167–178. http://dx.doi.org/10.1007/BF00268085

Pal, G., M.T. Paraz, and D.R. Kellogg. 2008. Regulation of Mih1/Cdc25 by protein phosphatase 2A and casein kinase 1. *J. Cell Biol.* 180:931–945. http://dx.doi.org/10.1083/jcb.200711014

Pereira, G., T. Höfken, J. Grindlay, C. Manson, and E. Schiebel. 2000. The Bub2p spindle checkpoint links nuclear migration with mitotic exit. *Mol. Cell*. 6:1–10.

Pruyne, D., L. Gao, E. Bi, and A. Bretscher. 2004. Stable and dynamic axes of polarity use distinct formin isoforms in budding yeast. *Mol. Biol. Cell*. 15:4971–4989. http://dx.doi.org/10.1091/mbc.E04-04-0296

Queralt, E., and F. Uhlmann. 2008. Separase cooperates with Zds1 and Zds2 to activate Cdc14 phosphatase in early anaphase. *J. Cell Biol.* 182:873–883. http://dx.doi.org/10.1083/jcb.200801054

Rahal, R., and A. Amon. 2008. Mitotic CDKs control the metaphase-anaphase transition and trigger spindle elongation. *Genes Dev.* 22:1534–1548. http://dx.doi.org/10.1101/gad.1638308

Robinson, L.C., M.M. Menold, S. Garrett, and M.R. Culbertson. 1993. Casein kinase I-like protein kinases encoded by YCK1 and YCK2 are required for yeast morphogenesis. *Mol. Cell. Biol.* 13:2870–2881.

Roelants, F.M., P.D. Torrance, and J. Thorner. 2004. Differential roles of PDK1- and PDK2-phosphorylation sites in the yeast AGC kinases Ypk1, Pkc1 and Sch9. *Microbiology*. 150:3289–3304. http://dx.doi.org/10.1099/mic.0.27286-0

Rossio, V., and S. Yoshida. 2011. Spatial regulation of Cdc55–PP2A by Zds1/Zds2 controls mitotic entry and mitotic exit in budding yeast. *J. Cell Biol.* 193:445–454. http://dx.doi.org/10.1083/jcb.201101134

Rupes, I. 2002. Checking cell size in yeast. *Trends Genet.* 18:479–485. http://dx.doi.org/10.1016/S0168-9525(02)02745-2

Russell, P., and P. Nurse. 1986. cdc25+ functions as an inducer in the mitotic control of fission yeast. *Cell*. 45:145–153. http://dx.doi.org/10.1016/0092-8674(86)90546-5

Russell, P., S. Moreno, and S.I. Reed. 1989. Conservation of mitotic controls in fission and budding yeasts. *Cell*. 57:295–303. http://dx.doi.org/10.1016/0092-8674(89)90967-7

Saka, A., M. Abe, H. Okano, M. Minemura, H. Qadota, T. Utsugi, A. Mino, K. Tanaka, Y. Takai, and Y. Ohya. 2001. Complementing yeast rho1 mutation groups with distinct functional defects. *J. Biol. Chem.* 276:46165–46171. http://dx.doi.org/10.1074/jbc.M103805200

Sakchaisri, K., S. Asano, L.R. Yu, M.J. Shulewitz, C.J. Park, J.E. Park, Y.W. Cho, T.D. Veenstra, J. Thorner, and K.S. Lee. 2004. Coupling morphogenesis to mitotic entry. *Proc. Natl. Acad. Sci. USA*. 101:4124–4129. http://dx.doi.org/10.1073/pnas.0400641101

Schmidt, A., J. Durgan, A. Magalhaes, and A. Hall. 2007. Rho GTPases regulate PRK2/PKN2 to control entry into mitosis and exit from cytokinesis. *EMBO J.* 26:1624–1636. http://dx.doi.org/10.1038/sj.emboj.7601637

Shulewitz, M.J., C.J. Inouye, and J. Thorner. 1999. Hsl7 localizes to a septin ring and serves as an adapter in a regulatory pathway that relieves tyrosine phosphorylation of Cdc28 protein kinase in *Saccharomyces cerevisiae*. *Mol. Cell. Biol.* 19:7123–7137.

Sreenivasan, A., and D. Kellogg. 1999. The elm1 kinase functions in a mitotic signaling network in budding yeast. *Mol. Cell. Biol.* 19:7983–7994.

Tang, Z., T.R. Coleman, and W.G. Dunphy. 1993. Two distinct mechanisms for negative regulation of the Wee1 protein kinase. *EMBO J.* 12:3427–3436.

TerBush, D.R., T. Maurice, D. Roth, and P. Novick. 1996. The Exocyst is a multiprotein complex required for exocytosis in *Saccharomyces cerevisiae*. *EMBO J.* 15:6483–6494.

Uetz, P., L. Giot, G. Cagney, T.A. Mansfield, R.S. Judson, J.R. Knight, D. Lockshon, V. Narayan, M. Srinivasan, P. Pochart, et al. 2000. A comprehensive analysis of protein-protein interactions in *Saccharomyces cerevisiae*. *Nature*. 403:623–627. http://dx.doi.org/10.1038/35001009

Watanabe, M., C.Y. Chen, and D.E. Levin. 1994. *Saccharomyces cerevisiae* PKC1 encodes a protein kinase C (PKC) homolog with a substrate specificity similar to that of mammalian PKC. *J. Biol. Chem.* 269:16829–16836.

Wicky, S., H. Tjandra, D. Schieltz, J. Yates III, and D.R. Kellogg. 2011. The Zds proteins control entry into mitosis and target protein phosphatase 2A to the Cdc25 phosphatase. *Mol. Biol. Cell*. 22:20–32. http://dx.doi.org/10.1091/mbc.E10-06-0487

Wu, L., and P. Russell. 1993. Nim1 kinase promotes mitosis by inactivating Wee1 tyrosine kinase. *Nature*. 363:738–741. http://dx.doi.org/10.1038/363738a0

Xu, H., G.L. Boulianne, and W.S. Trimble. 2002. Membrane trafficking in cytokinesis. *Semin. Cell Dev. Biol.* 13:77–82. http://dx.doi.org/10.1016/S1084-9521(02)00012-5

Yamochi, W., K. Tanaka, H. Nonaka, A. Maeda, T. Musha, and Y. Takai. 1994. Growth site localization of Rho1 small GTP-binding protein and its involvement in bud formation in *Saccharomyces cerevisiae*. *J. Cell Biol.* 125:1077–1093. http://dx.doi.org/10.1083/jcb.125.5.1077

Yang, H., W. Jiang, M. Gentry, and R.L. Hallberg. 2000. Loss of a protein phosphatase 2A regulatory subunit (Cdc55p) elicits improper regulation of Swe1p degradation. *Mol. Cell. Biol.* 20:8143–8156. http://dx.doi.org/10.1128/MCB.20.21.8143-8156.2000

Yasutis, K., M. Vignali, M. Ryder, F. Tameire, S.A. Dighe, S. Fields, and K.G. Kozminski. 2010. Zds2p regulates Swe1p-dependent polarized cell growth in *Saccharomyces cerevisiae* via a novel Cdc55p interaction domain. *Mol. Biol. Cell*. 21:4373–4386. http://dx.doi.org/10.1091/mbc.E10-04-0326